

Transformation of the X-33 Strain of *Pichia pastoris* and the Small Scale Expression of  
the N103H Mutant Hen Egg White Lysozyme Gene

By

Praneeth Samalla

Submitted in Partial Fulfillment of the Requirements

for the Degree of

Master of Science

in the

Chemistry

Program

YOUNGSTOWN STATE UNIVERSITY

May, 2015

Transformation of the X-33 Strain of *Pichia pastoris* and the Small Scale Expression of  
the N103H Mutant Hen Egg White Lysozyme Gene

Praneeth Samalla

I hereby release this thesis to the public. I understand that this thesis will be made available from the OhioLINK ETD Center and the Maag Library Circulation Desk for public access. I also authorize the University or other individuals to make copies of this thesis as needed for scholarly research.

Signature:

---

*Praneeth Samalla*, Student

Date

Approvals:

---

*Dr. Michael A. Serra*, Thesis Advisor

Date

---

*Dr. Timothy R. Wagner*, Committee Member

Date

---

*Dr. Jonathan Caguiat*, Committee Member

Date

---

Dr. Salvatore A. Sanders, Associate Dean of Graduate Studies

Date

## ABSTRACT

Reactive oxygen species (ROS) are molecules or radicals which are produced from oxygen. Most ROS are highly reactive due to the presence of unpaired electrons in their valence shell. Metal ions such as  $\text{Fe}^{2+}$  or  $\text{Cu}^+$  are used as reducing agents in metal catalyzed oxidation (MCO) systems that generate the hydroxyl radical in a reaction with hydrogen peroxide. To study the oxidation of proteins by MCO systems a N103H mutant of hen egg white lysozyme (HEWL) was generated. The HEWL mutant N103H gene was successfully cloned into the pPICZ $\alpha$ A plasmid and subsequently transformed into Mach1<sup>TM</sup>-T1<sup>R</sup> chemically competent *Escherichia coli*. The recombinant plasmid was isolated, linearized, and transformed into the X-33 strain of the yeast *Pichia pastoris* by electroporation. Small scale expression was performed using a buffered glycerol media and methanol media at pH 6.0 and 7.0 for 4 days. Expression in unbuffered media was also performed. SDS-PAGE analysis of the supernatant samples from small scale expression revealed extracellular expression of a protein of the right size in a buffered medium whereas unbuffered medium showed no evidence of the expression of any proteins. Small scale expression in buffered media at pH 7.0 with antifoam appeared to give the best protein expression. A Bradford assay indicated the extracellular expression of protein to a concentration of about 0.1 mg/mL. Enzyme assays of pooled and concentrated fractions collected over four days showed no lysozyme activity. A low concentration of the N103H HEWL mutant might be the reason for no activity.

## ACKNOWLEDGEMENTS

I would like to thank my advisor Dr. Michael Serra for his constant support and guidance throughout this project. He was always helpful and guided me through the coursework, without him this wouldn't be possible for me. I would also like to thank Dr. Timothy R. Wagner and Dr. Jonathan Caguiat for their time to be on my thesis committee and their helpful comments throughout writing this thesis. I also extend my gratitude to other members of the Serra Research Group for their constant support. I would like to thank Youngstown State University Department of Chemistry for supporting this project.

I would like to thank the professors of the Chemistry and Biology Departments for their advice and access to their equipment round the clock which made this thesis possible. I owe a great deal of gratitude to my friends Dr. Pavan Maheshwaram, Dr. Dhruthiman Mantheni for their constant support.

Finally, I would like to extend my deepest gratitude to my mom, Samalla Jamuna and all my family members for their love and support during my stay at YSU. They always lifted up my spirits and encouraged me without which this thesis wouldn't have been possible.

## TABLE OF CONTENTS

Title Page.....	i
Signature page.....	ii
Abstract.....	iii
Acknowledgements.....	iv
Table of Contents.....	v
List of Figures.....	viii
List of Equations.....	x
List of Tables.....	xi
List of Abbreviations.....	xii
Chapter 1: Introduction.....	1
Reactive Oxygen Species.....	1
Oxidative Damage.....	3
Metal Catalyzed Oxidation Systems.....	4
Site Specific Oxidation.....	4
Protein Oxidation.....	7
Anti-Oxidant Defense Systems.....	10
Disorders.....	11
Lysozyme.....	12
<i>Pichia pastoris</i> and pPICZ $\alpha$ A.....	14
Statement of the Research Problem.....	15
Chapter 2: Materials and Methods.....	17
Materials and Instrumentation.....	17

Preparation of Yeast Vector pPICZ $\alpha$ A <sup>®</sup> Plasmid for Ligation.....	18
Linearization of pPICZ $\alpha$ A Plasmid.....	18
Ligation of N103H Gene into Linearized pPICZ $\alpha$ A Plasmid.....	19
Confirmation of Ligation of the Mutant Genes into pPICZ $\alpha$ A Plasmid.....	20
Linearization of <i>hewl</i> -N103H-pPICZ $\alpha$ A for Yeast Transformation.....	20
Preparation of Competent Cells.....	21
Transformation of Yeast.....	21
Confirmation of Yeast Transformation by the Polymerase Chain Reaction.....	22
Expression of Mutant Proteins.....	24
Analysis of Mutant Proteins.....	25
SDS-PAGE.....	25
Bradford Assay.....	26
Enzyme Assay.....	26
Chapter 3: Results.....	28
Preparation of Yeast Vector pPICZ $\alpha$ A <sup>®</sup> for Ligation.....	28
Linearization of pPICZ $\alpha$ A Plasmid.....	28
Ligation of N103H Gene into Linearized pPICZ $\alpha$ A for Ligation.....	29
Confirmation of Ligation reaction.....	30
Linearization of <i>hewl</i> -N103H-pPICZ $\alpha$ A for Yeast Transformation.....	31
Preparation of Competent <i>Pichia pastoris</i> cells.....	32
Growth of Yeast after Electroporation.....	33
Confirmation of Yeast Transformation by the Polymerase Chain Reaction.....	35
Analysis of Mutant Proteins.....	37

SDS-PAGE.....	37
Bradford Assay.....	43
Enzyme Assay.....	46
Chapter 4: Discussion.....	47
Chapter 5: Conclusion.....	50
References.....	51

## List of Figures

1.1: Site specific metal catalyzed oxidation of protein amino acid residues.....	6
1.2: Metal catalyzed oxidation of proteins.....	7
1.3: Oxygen free radical mediated oxidation of proteins.....	8
1.4: Protein cleavage by diamide and $\alpha$ -amide pathways.....	10
1.5: Mechanism of oxidative tissue damage leading to pathological conditions .....	11
1.6: Primary sequence of lysozyme enzyme.....	12
1.7: Cleavage specificity of lysozyme enzyme.....	13
1.8: Double displacement reaction of lysozyme enzyme.....	14
1.9: pPICZ $\alpha$ <sup>®</sup> vector.....	15
1.10: 3-D model of native HEWL enzyme.....	16
3.1: A gel image of pPICZ $\alpha$ A plasmid DNA.....	28
3.2: A gel image of linearized pPICZ $\alpha$ A plasmid DNA.....	29
3.3: A gel image of ligated <i>hewl</i> -N103H-pPICZ $\alpha$ A plasmid DNA.....	30
3.4: A gel image of double digest of <i>hewl</i> -N103H-pPICZ $\alpha$ A plasmid DNA.....	31
3.5: A gel image of linearized <i>hewl</i> -N103H-pPICZ $\alpha$ A plasmid DNA.....	32
3.6: A picture of the two strains of <i>P. pastoris</i> used for electroporation.....	33
3.7: Picture of transformed X-33 with <i>hewl</i> -N103H-pPICZ $\alpha$ A plasmid DNA.....	34
3.8: Picture of transformed X-33 <i>hewl</i> -N103H-pPICZ $\alpha$ A plasmid DNA re-streaked on YPD plates.....	34
3.9: A gel image of genomic DNA from transformed X-33 yeast.....	36
3.10: A gel image of PCR analysis of X-33 transformed yeast DNA.....	36
3.11: SDS-PAGE of supernatant samples at pH 6.0.....	37
3.12: SDS-PAGE of supernatant samples at pH6.0 and 7.0 with anti-foam.....	39



3.13: A graph showing plot of Log. Mol. Wt. vs Rf values.....	40
3.14: SDS-PAGE of supernatant samples of controls.....	41
3.15: SDS-PAGE of supernatant samples of unbuffered media.....	42
3.16: A graph showing plot of Absorbance (595nm) vs concentration of BSA (24 hr pooled samples).....	44
3.17: A graph showing plot of Absorbance (595nm) vs concentration of BSA (pooled samples).....	45

## List of Equations

1.1: Reduction of Oxygen to Water.....	1
1.2: The Fenton Reaction.....	2
1.3: Haber-Weiss Equation.....	2

## List of Tables

1.1: List of common MCO systems.....	4
1.2: Amino acids and their products of oxidation.....	9
2.1: Preparation of samples for Bradford Assay.....	26
3.1: Calculation of Rf values for each gel.....	40
3.2: Bradford Assay of the pooled 24 hr samples.....	43
3.3: Calculated concentration of the pooled 24 hr samples by Bradford Assay.....	44
3.4: Bradford Assay of the pooled samples.....	45
3.5: Calculated concentration of the pooled samples by Bradford Assay.....	46
3.6: Assay results of the supernatant samples.....	46

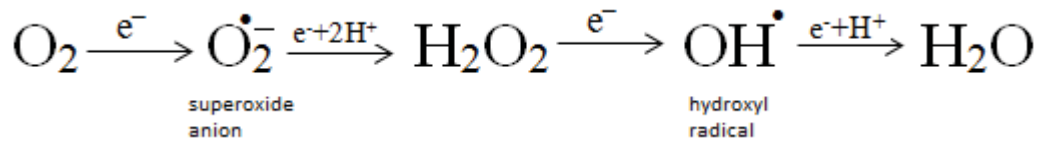
## List of Abbreviations

μg	Microgram
μL	Microliter
μM	Micro molar
bp	Base pair
kbp	Kilo base pair
BSA	Bovine serum albumin
DDI	Distilled De-ionized water
DNA	Deoxyribonucleic acid
RNA	Ribonucleic acid
EDTA	Ethylenediaminetetraacetic acid
mg	Milligram
ng	Nanogram
PAGE	Poly acrylamide gel electrophoresis
SDS	Sodium dodecyl sulfate
U/mL	Units per milliliter
V	Volts
UV-Vis	Ultraviolet-visible
LB	Luria-Bertini
HEWL	Hen egg white lysozyme
DTT	Dithiotheritol
NADPH	Nicotinamide adenine dinucleotide phosphate
NADH	Nicotinamide adenine dinucleotide
YNB	Yeast nitrogen base

## CHAPTER 1: INTRODUCTION

### *Reactive Oxygen Species*

Reactive oxygen species (ROS) are molecules or radicals produced from the reduction of oxygen.<sup>1</sup> Most ROS are highly reactive due to the presence of unpaired electrons in their valence shell.<sup>2</sup> Equation 1.1 shows the univalent reduction of O<sub>2</sub> which results in the formation of superoxide anion (O<sub>2</sub><sup>•-</sup>), H<sub>2</sub>O<sub>2</sub> and the hydroxyl radical (OH<sup>•</sup>).<sup>1</sup>



Equation 1.1: The four electron reduction of oxygen to water produces the ROS superoxide anion, hydrogen peroxide, and the hydroxyl radical.<sup>1</sup>

ROS are produced during changes in intra and extra-cellular conditions of normal cellular metabolism.<sup>3</sup> Exogenous ROS are formed by external factors such as ionizing radiation, smoke, and drugs.<sup>2</sup> Endogenous ROS are produced by internal factors and include NADPH oxidase complexes in cell membranes, in mitochondria by electron leakage from the electron transport chain, in peroxisomes and in endoplasmic reticulum (hypoxia/ischemia).

Most ROS are produced in cells by the respiratory chain in mitochondria. The univalent reduction of O<sub>2</sub> in respiring cells is normally restricted by cytochrome oxidase of the electron transport chain in mitochondria. The cytochrome oxidase reduces molecular oxygen by four electrons to H<sub>2</sub>O without any release of O<sub>2</sub><sup>•-</sup> or H<sub>2</sub>O<sub>2</sub>. A leak of a single electron at a specific site, e.g. ubisemiquinone or ubiquinone, of the mitochondrial electron transport chain results in the single electron reduction of O<sub>2</sub> producing the superoxide ion (O<sub>2</sub><sup>•-</sup>). Cytochrome P-450 reductase and cytochrome b-5

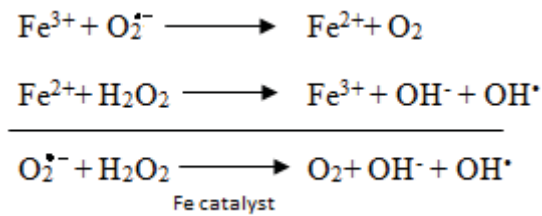
reductase may generate  $O_2^{\bullet -}$  and  $H_2O_2$  in the endoplasmic reticulum during their catalytic cycles. Activation of NADPH oxidase generates superoxide anion ( $O_2^{\bullet -}$ ) and  $H_2O_2$  during phagocytosis.<sup>1</sup>

The production of the hydroxyl radical *in vivo* requires the presence of trace amounts of transition metal ions like iron or copper. The Fenton reaction illustrates the reduction of  $H_2O_2$  in the presence of  $Fe^{2+}$  (Equation 1.2).<sup>4</sup>



Equation 1.2: The Fenton reaction results in the reduction of hydrogen peroxide by  $Fe^{2+}$  into the hydroxyl ion and the hydroxyl radical.<sup>4</sup>

The Haber-Weiss reaction is a two-step reaction whereby a metal ion in a higher oxidation state is reduced by the superoxide anion. This is followed by the subsequent oxidation of the metal ion and reduction of  $H_2O_2$  giving the hydroxyl ion and the hydroxyl radical (Equation 1.3).<sup>5</sup>



Equation 1.3: The Haber-Weiss reaction shows the reduction of  $Fe^{3+}$  ion by the superoxide anion followed by the Fenton reaction resulting in formation of the hydroxyl ion and the hydroxyl radical. The overall reaction can be summarized as a reduction of hydrogen peroxide by superoxide anion in the presence of iron as catalyst.<sup>5</sup>

### ***Oxidative Damage***

Vital cell components such as polyunsaturated fatty acids, proteins, and nucleic acids are subject to oxidative damage by ROS. This damage results in alteration of intrinsic properties like fluidity, ion transport, loss of enzyme activity, protein cross linking, inhibition of protein synthesis and DNA damage, which ultimately results in cell death.<sup>1</sup> Some of the well-known consequences of ROS include DNA strand scission, nucleic acid base modification, protein oxidation and lipid peroxidation.<sup>1</sup> Oxygen radicals catalyze the oxidative modification of lipids. Methylene groups that are adjacent to double bonds in polyunsaturated fatty acids are weaker which makes them vulnerable to abstraction of their hydrogen. Oxidative damage in mitochondrial DNA results in formation of abnormal components of the electron transport chain which further increases leakage of electrons, eventually leading to cell damage that promote cancer and the aging process.<sup>6</sup>

Free radicals produced during electron transport can stimulate protein degradation. Oxidative damage of proteins by metabolic processes leads to degradation of damaged proteins and promotes the synthesis of a new proteins.<sup>3</sup> Extensive studies on aging processes established the fact that an increase in concentration of the catalytically inactive, less active and more thermolabile forms of enzymes in cells during aging also showed increased levels of protein carbonyl content.<sup>3</sup> Levels of glyceraldehyde-3-phosphate dehydrogenase, aspartate amino transferase, and phosphoglycerate kinase decline with age. Oxidative damage to proteins also results in an increase of protein carbonyl content.<sup>7</sup>

### ***Metal Catalyzed Oxidation (MCO) Systems***

MCO-mediated protein oxidation is an indicator of tissue damage. Pathological conditions in both human and animal models noticed the formation of protein carbonyl derivatives. During the period of oxidative burst in some endogenous neutrophil proteins there is an increase in carbonyl content and endogenous enzymes are inactivated. This results in activation of neutrophils at extravascular sites further resulting in protein oxidation and tissue damage.<sup>9</sup>

Metal-ion catalyzed oxidation may also cause atherosclerosis where oxidation of low density lipoproteins by endothelial cells and subsequent uptake of oxidized LDL by monocytes/macrophages is one of the events in atherogenesis. Modification of apoprotein B includes fragmentation of the polypeptide and loss of lysyl, prolyl, and histidyl residues which are characteristics of MCO reactions.<sup>10</sup> Table 1.1 lists some common MCO systems.<sup>9</sup>

Table 1.1: List of Common MCO Systems.

Non-enzymatic MCO systems	Enzymatic MCO systems
Oxygen and Ferric ion	Fe(III)/O <sub>2</sub> /NADPH oxidase
Oxygen and Ferrous ion	Fe(III)/O <sub>2</sub> /NADH oxidase
Ascorbate, Oxygen and Ferrous ion	Fe(III)/O <sub>2</sub> /Xanthine oxidase
Hydrogen peroxide and Ferrous ion	Fe(III)/O <sub>2</sub> /Cytochrome P-450 reductase
Ascorbate, Oxygen and Cupric ion	
Hydrogen peroxide and Cupric ion	

### ***Site Specific Oxidation***

Free amino acids and amino acid residues in proteins are susceptible to oxidation by MCO systems. Studies with *E. coli* glutamine synthetase found that amino acid



residues situated at metal binding sites on the enzyme are uniquely sensitive to metal oxidation by a site specific mechanism.<sup>12</sup> Metal catalyzed oxidation of proteins which involves the interaction of H<sub>2</sub>O<sub>2</sub> and metal ions Fe(II) or Cu(I) at the metal binding sites on the protein is a site specific process.<sup>13</sup> The site specific nature of the reaction is illustrated by the following: (a) inactivation of enzymes by MCO systems is relatively insensitive to inhibition by free radical scavengers, (b) only one or a few amino acids residue in a protein can be modified by MCO system, (c) most of the enzymes that are sensitive to modification by MCO systems require metal ions for catalytic activity; therefore, they must contain a metal ion binding site, and (d) the loss of catalytic activity in *E. coli* glutamine synthetase is correlated with the loss of a single arginyl residue per subunit, both of which are situated in close proximity to one of two divalent metal binding sites on the enzyme.

An example of site-specific oxidation involving a lysyl residue and Fe(II) is shown in Figure 1.1. In step 1 Fe(II) forms a chelate complex by binding with the side chain amino group of a lysyl residue. In step 2 the complex reacts with H<sub>2</sub>O<sub>2</sub> generating the hydroxyl radical, this is followed by hydrogen abstraction forming a carbon centered free radical (step 3). In step 4, the addition of a proton results in formation of an imine intermediate which further results in formation of a 2-aminoadipic semialdehyde residue (step 5).

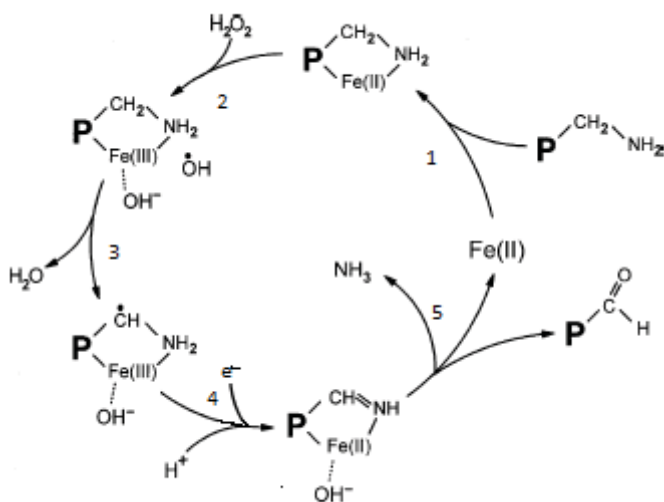


Figure 1.1: An example of site specific oxidation of a lysyl residue by Fe(II) resulting in the formation of a 2-amino-adipic-semialdehyde residue.<sup>12</sup>

MCO systems include enzymatic systems such as Fe(III)/O<sub>2</sub>/NADPH and NADH oxidase systems. Non-enzymatic MCO systems include Fe(III)/O<sub>2</sub>/ascorbate. Figure 1.2 depicts the ability of MCO systems to catalyze the reduction of O<sub>2</sub> to H<sub>2</sub>O<sub>2</sub> and the reduction of Fe(III) to Fe(II) by both O<sub>2</sub><sup>•-</sup> dependent and O<sub>2</sub><sup>•-</sup> independent pathways. The sequence in Figure 1.2 shows that the production of H<sub>2</sub>O<sub>2</sub>, which is a normal product of oxidase catalyzed reactions, occurs by the dismutation of O<sub>2</sub><sup>•-</sup> produced as a byproduct of electron transport.<sup>13</sup>

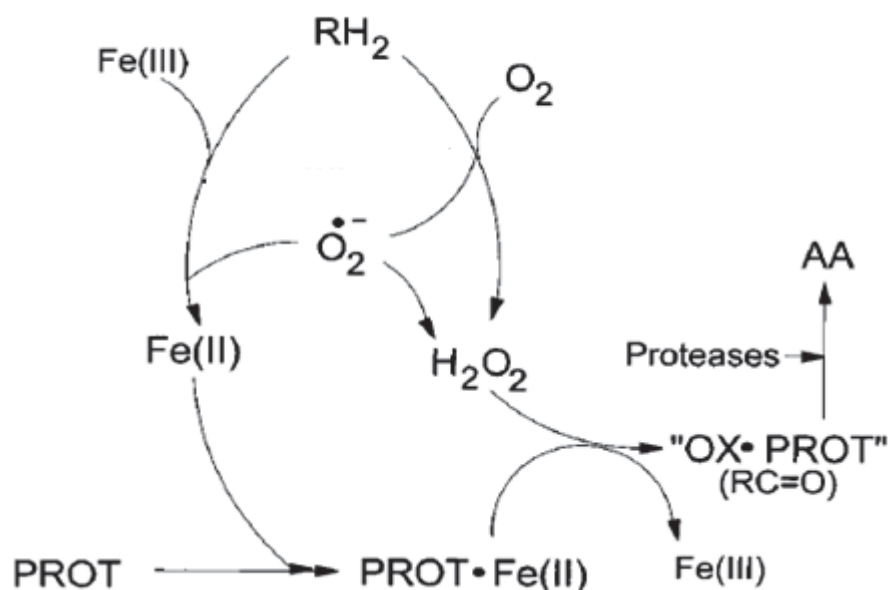


Figure 1.2: In this reaction reduction of Fe(III) to Fe(II) occurs both by  $O_2^{\bullet-}$  dependent and  $O_2^{\bullet-}$  independent pathways.  $RH_2$  stands for electron donors (NADH, NADPH), OX-PROT- oxidized protein, PROT-protein, AA- amino acids.<sup>13</sup>

### ***Protein Oxidation***

ROS can lead to oxidation of amino acid residue side chains, formation of protein-protein cross linkages, and oxidation of the protein backbone resulting in protein fragmentation. In Figure 1.3 oxidation of the protein backbone begins with a  $OH^{\bullet}$  dependent abstraction of the  $\alpha$ -hydrogen atom of an amino acid residue resulting in the formation of a carbon-centered radical which further initiates oxidative attack of the polypeptide backbone.<sup>6</sup> For this reaction to occur, the  $OH^{\bullet}$  radical is generated by radiolysis of water or by metal catalyzed cleavage of  $H_2O_2$ . The carbon centered radical which is formed reacts rapidly with  $O_2$  to form an alkylperoxyl radical which gives rise to the alkylperoxide. The alkylperoxide can be converted to an alkoxyl radical, which is further converted to a hydroxyl protein derivative. Many of the significant steps in this pathway are mediated by interactions with  $HO_2^{\bullet}$  and can be catalyzed by  $Fe^{2+}$  or by  $Cu^+$ .<sup>6</sup>

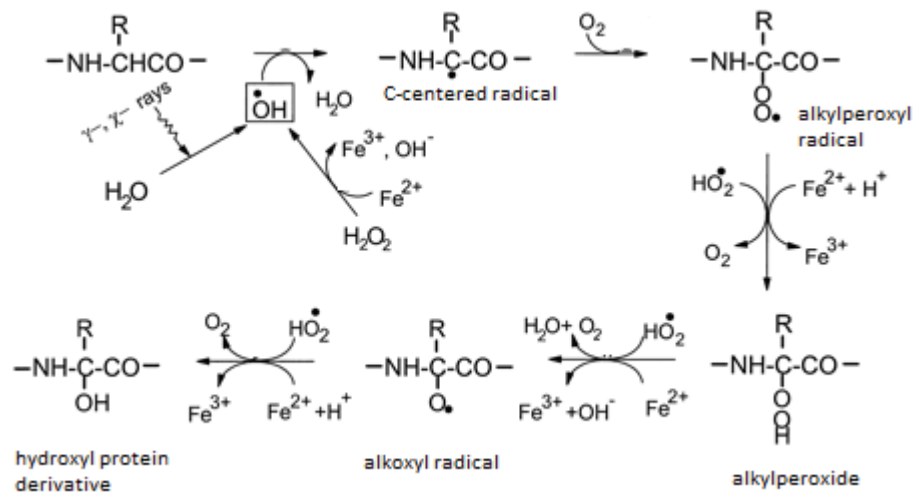


Figure 1.3: Oxygen free radical-mediated oxidation of proteins. In this reaction the generated  $\text{OH}^\bullet$  radical results in abstraction of the  $\alpha$ -hydrogen which reacts with  $\text{O}_2$  to form an alkylperoxyl radical. The alkylperoxyl radical can be converted to an alkylperoxide followed by the alkoxy radical and to alkoxy radical leading to formation of a hydroxyl protein derivative.<sup>6</sup>

Cysteine and methionine residues are highly susceptible to oxidation by ROS. Mild oxidizing conditions will generate disulfide bonds between cysteine residues. Methionine residues are oxidized to methionine sulfoxide residues. Aromatic amino acids also undergo oxidation by ROS. For example, tryptophan is oxidized to formylkynurenine and kynurenine. Histidine residues are converted to 2-oxohistidine, asparagine and aspartic acid residues. Table 1.2 shows the amino acids and their oxidation products. Cysteine and methionine residues of proteins are vulnerable to oxidation by peroxynitrate as well.<sup>6</sup>

Table 1.2: Amino acids and their products of oxidation.<sup>6</sup>

Amino acids	Oxidation products
Cysteine	Disulfides, cysteic acid
Methionine	Methionine sulfoxide, methionine sulfone
Tryptophan	2-, 4-, 5-, 6-, and 7-Hydroxytryptophan, nitrotryptophan, kynurenine, 3-hydroxykynurinine, formylkynurinine
Phenylalanine	2,3-Dihydroxyphenylalanine, 2-, 3-, and 4-hydroxyphenylalanine
Tyrosine	3,4-Dihydroxyphenylalanine, tyrosine-tyrosine cross-linkages, Tyr-O-Tyr, cross-linked nitrotyrosine
Histidine	2-Oxohistidine, asparagine, aspartic acid
Arginine	Glutamic semialdehyde
Lysine	$\alpha$ -Aminoadipic semialdehyde
Proline	2-Pyrrolidone, 4- and 5-hydroxyproline pyroglutamic acid, glutamic semialdehyde
Threonine	2-Amino-3-ketobutyric acid
Glutamyl	Oxalic acid, pyruvic acid

Protein carbonyl derivatives increase with oxidative damage by direct oxidation of amino acid side chains or by reaction with aldehydes. Carbonyl derivatives serve as a biomarker of oxidative damage. Oxidative cleavage of proteins by the  $\alpha$ -amidation pathway or by oxidation of glutamyl side chain leads to formation of a peptide in which the N-terminal amino acid is blocked by a  $\alpha$ -ketoacyl derivative. Table 1.2 shows that direct oxidation of lysyl, arginyl, prolyl and threonyl residues yield carbonyl derivatives. Carbonyl groups sometimes may be introduced into proteins by reactions with aldehydes which are produced during lipid peroxidation.<sup>6</sup>

Oxidation of proteins by ROS can lead to the cleavage of peptide bonds. Alkoxy radicals and alkylperoxide derivatives of proteins can undergo cleavage by either the  $\alpha$ -amidation pathway or the diamide pathway. In the  $\alpha$ -amidation pathway (Figure 1.4 b), the C-terminal residue of the fragment derived from the N-terminal region of the protein exists as an amide derivative, and the N-terminal residue derived from C-terminal portion

of protein will exist as an  $\alpha$ -keto-acyl derivative. In the diamide pathway (Figure 1.4 a), the C-terminal residue derived from the N-terminal portion of the protein will exist as a diamide derivative and the N-terminal residue from the C-terminal region exists as an iso-cyanate derivative. Oxidation of glutamyl and aspartyl residues of proteins can also lead to peptide bond cleavage.<sup>6</sup>

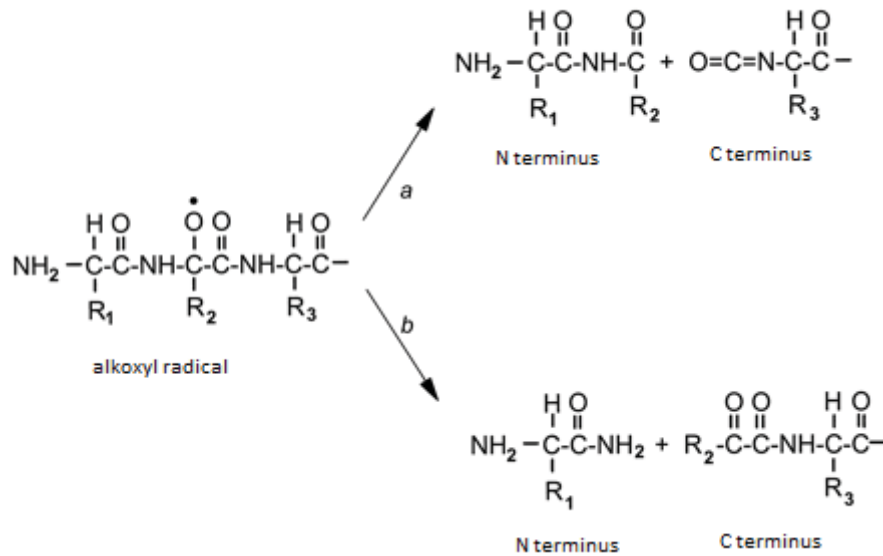


Figure 1.4: Protein cleavage by the diamide pathway (a) and the  $\alpha$ -amidation pathway (b).<sup>6</sup>

### ***Anti-oxidant Defense Systems***

An anti-oxidant is a molecule that inhibits the oxidation of other molecules. On the other hand, pro-oxidants are chemicals that induce oxidative stress, either by generating reactive oxygen species or by inhibiting anti-oxidant systems. Pro-oxidants can include free radical containing molecules in cells or tissues. In the presence of transition metals, anti-oxidants such as flavonoids act as pro-oxidants.<sup>1</sup>

To mitigate oxidative damage, anti-oxidant defense mechanisms have evolved over time. Anti-oxidants are the first line of defense to protect the body from oxidative

stress. Endogenous anti-oxidant defenses include anti-oxidant enzymic and non-enzymic molecules that are distributed within the cytoplasm and organelles of the cell. Primary anti-oxidant enzymes include superoxide dismutase, catalase and several peroxidases, that catalyze complex reactions which involve the conversion of ROS into more stable molecules. Non-enzymatic anti-oxidants include such compounds as glutathione, NADPH, thioredoxin, and vitamins E and C which all act as direct scavengers of ROS.<sup>3</sup>

**Disorders**

A decrease in cellular anti-oxidant systems or elevated levels of ROS leads to several pathological conditions. Disorders such as rheumatoid arthritis, hemorrhagic shock, cardiovascular diseases, gastro-intestinal ulcerogenesis and AIDS are some of the examples for ROS-mediated disorders.<sup>7</sup>

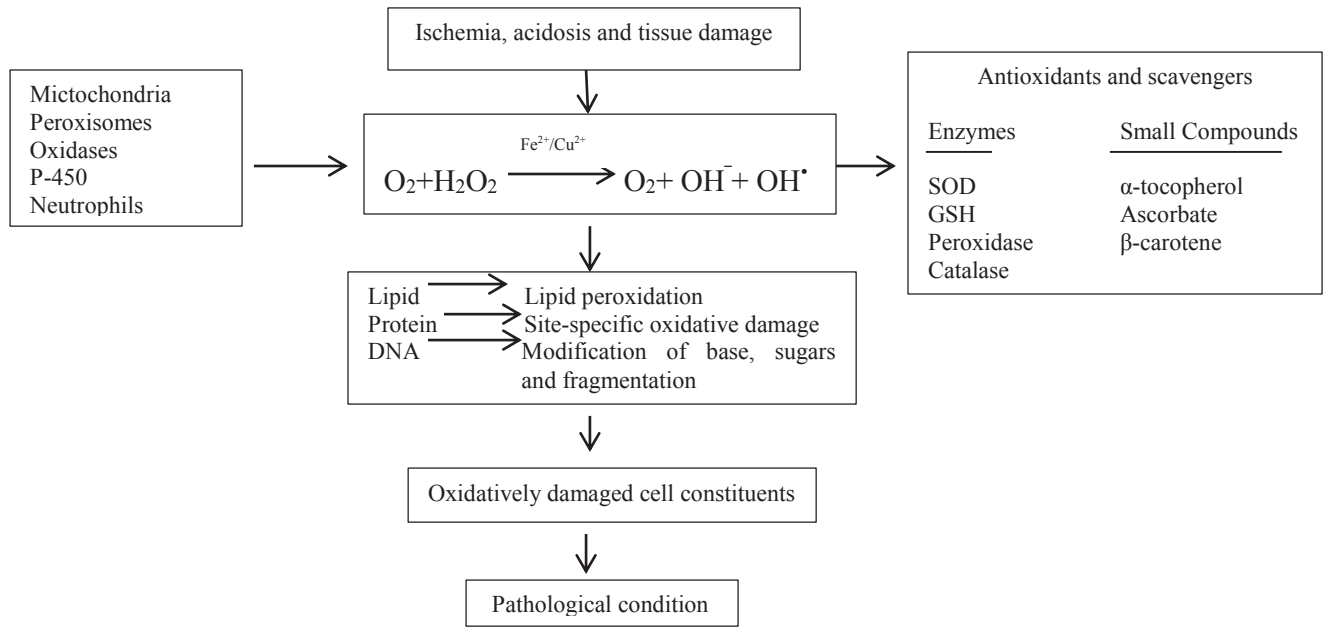


Figure 1.5: A scheme illustrating the mechanism of the oxidative tissue damage leading to pathological conditions.<sup>1</sup>





HEWL is a bactericidal enzyme that catalyzes the hydrolysis of  $\beta$  (1 $\rightarrow$ 4) glycosidic linkages between N-acetylmuramic acid (NAM) and N-acetylglucosamine (NAG) in the NAM-NAG component of the cell wall peptidoglycans of bacteria, especially gram positive bacteria (Figure 1.7).<sup>19</sup>

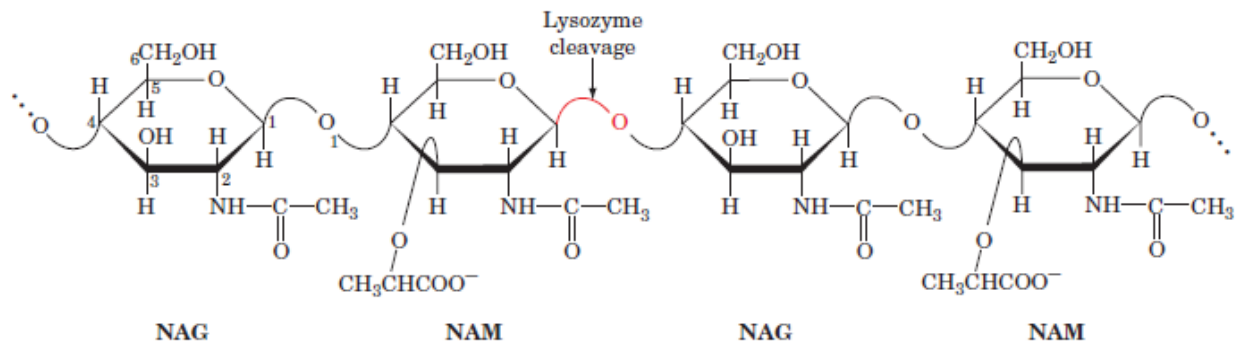


Figure 1.7: The alternating NAG and NAM peptidoglycans of bacterial cell wall showing cleavage specificity of Lysozyme.<sup>19</sup>

The hydrolytic reaction of lysozyme occurs through a double displacement reaction. Lysozyme attaches to the bacterial cell wall by binding to the polysaccharide unit (Figure 1.8 step 1). Glu 35 transfers a proton to the oxygen atom linking D and E residues rings cleaving the  $\beta$  (1 $\rightarrow$ 4) glycosidic bond (Figure 1.8 step 2). The carboxylate group of Asp 52 nucleophilically attacks C1 of the D-ring forming a covalent glycosyl intermediate (Figure 1.8 step 3). Water replaces the E-ring product at the active site, followed by hydrolysis of the covalent bond in the presence of Glu 35 releasing the D-ring product.<sup>19</sup>

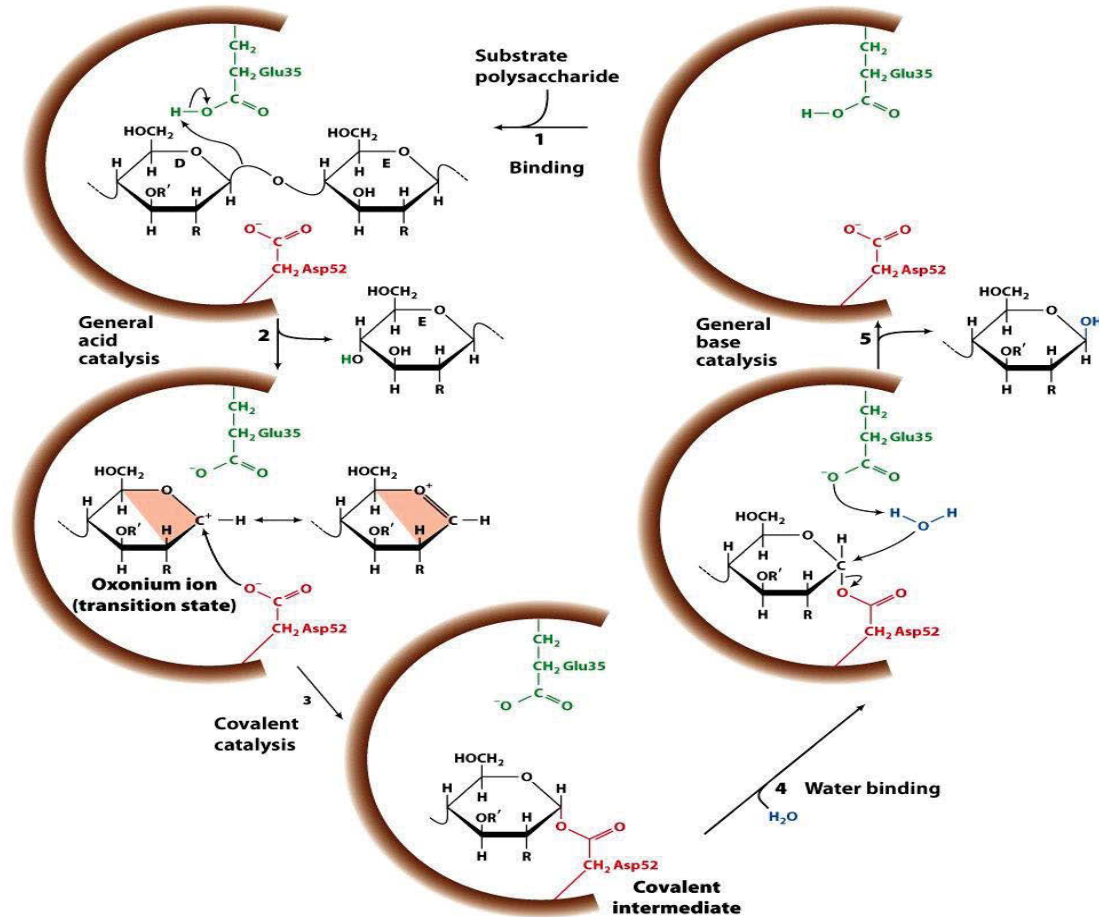


Figure 15-14  
© John Wiley & Sons, Inc. All rights reserved.

Figure 1.8: The double displacement catalytic mechanism of HEWL. In this reaction Glu 35 acts as an acid catalyst, it also acts as a base by abstracting a proton from  $H_2O$  and Asp 52 acts as covalent catalyst.<sup>19</sup>

### *Pichia pastoris* and pPICZαA<sup>®</sup>

*Pichia pastoris* is a species of methylotrophic yeast which was chosen for protein expression. *P. pastoris* is as easy to manipulate as *E. coli*. It is less expensive compared to baculovirus or mammalian tissue cultures, and it has higher expression levels.

pPICZαA is a *P. pastoris* vector for methanol-inducible expression of a secreted protein (Figure 1.9). This plasmid confers Zeocin<sup>™</sup> resistance as a selective marker. It has an α-factor signal sequence for extracellular expression of the gene product. A 5'

*AOX1* site allows over-expression of the recombinant gene when placed behind the alcohol oxidase gene promoter with methanol as the sole source of carbon.

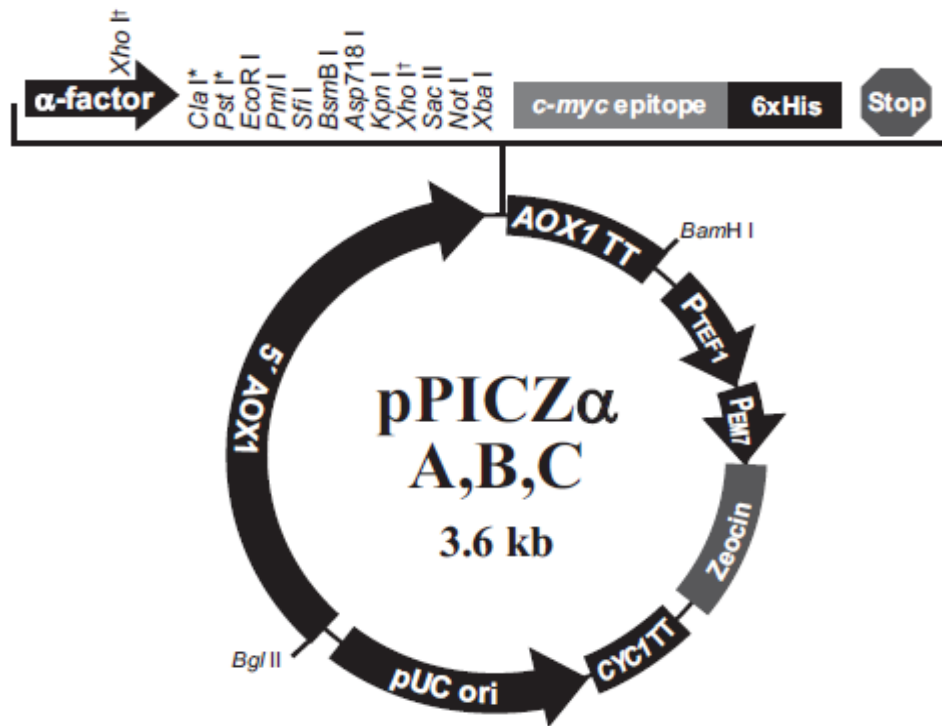


Figure 1.9: A picture of the pPICZ $\alpha$  plasmid showing its important features including, the  $\alpha$ -factor signal sequence for extracellular expression, 5'*AOX1* promote methanol induced high level expression of recombinant protein, and the gene that confers Zeocin<sup>TM</sup> resistance.

### ***Statement of Research Problem***

A “caged” reaction occurs when a hydroxyl radical is generated in a protective pocket on a protein in a reaction between a bound metal ion and H<sub>2</sub>O<sub>2</sub>. The free radical reacts with susceptible amino acids in the binding site. Caged reactions indicate that the tertiary structure of a protein may play a crucial role in determining the sites of oxidative damage in a protein. On the other hand, it is known that certain amino acids such as histidine have a high affinity for metal ions. Perhaps primary structure is the primary determinant for site specific oxidation using MCO systems. The main aim of this research

is to investigate the oxidation of a mutant lysozyme using a copper(II)/ hydrogen peroxide MCO system as a means to investigate the relationship between protein structure and oxidative damage. The N103H mutant of HEWL was used in this study. The histidine residue incorporated at position 103 is found on the surface of the protein thereby creating two histidyl residues that are in different environments in the protein. The naturally occurring histidine is found at position 15 in the primary sequence, and it is partially buried in a pocket of the protein (Figure 1.10). The presence of two histidyl residues provides a means to investigate the effect of tertiary structure on the nature and extent of site-specific oxidative damage. This research involves the ligation of the mutant gene into the yeast plasmid vector pPICZ $\alpha$ A. The recombinant DNA was transformed into the X-33 strain *Pichia pastoris* and conditions for the small scale expression of the N103H mutant lysozyme were examined.

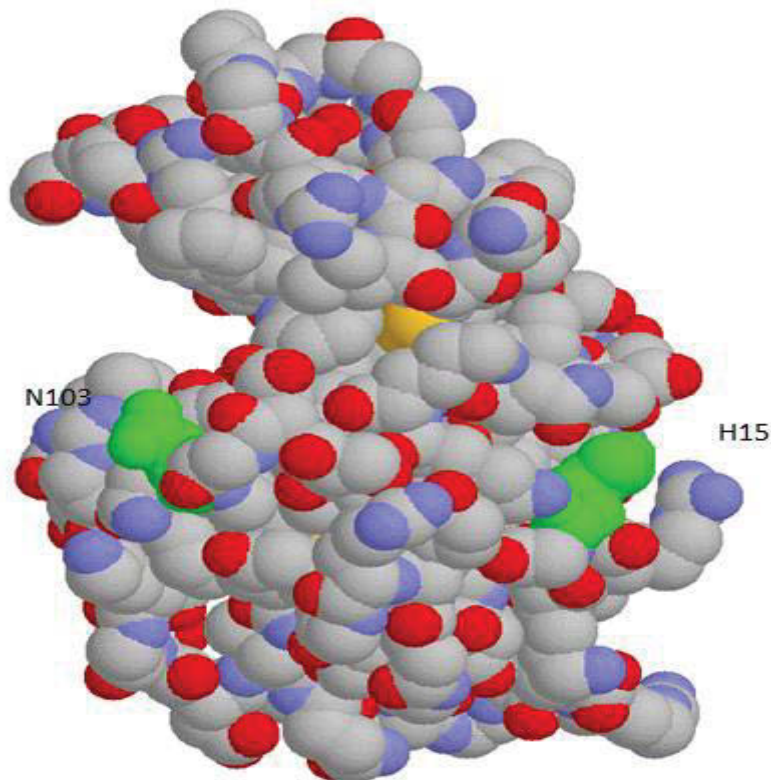


Figure 1.10: A Three-dimensional model of native HEWL showing histidine at position 15 which is partially buried in the pocket and asparagine at 103 exposed to the surface of the protein.

## CHAPTER 2: MATERIALS AND METHODS

### *Materials and Instrumentation*

Agar, agarose, glycerol, tryptone, yeast extract, 100 bp DNA ladder, 1 kbp DNA ladder, Tris-Hydroxymethyl amino methane (THAM), TAE buffer and the Cyclo Pure™ Agarose Gel Extraction Kit were purchased from Amresco. pH measurements were determined using an Accumet Digital pH meter from Fischer Scientific. A Technegene version 10.19 thermo cycler was used to perform PCR analysis. Dextrose, sodium chloride, EDTA, sodium acetate, and ethidium bromide were purchased from Fisher Scientific. A Mettler AE100 was used for all mass measurements. An Agilent 8453 UV-Vis spectrophotometer manufactured by Hewlett Packard operating with the UV-Visible Chemstation software suite was used for all spectrophotometric analysis. Acetone, acetic acid, methanol, ethanol and isopropyl alcohol was purchased from Pharmaco-AAPER. 2 mm magnetic stir bars, 3 mL glass cuvette used for kinetic analysis were purchased from Fisher Scientific. A Tuttnauer 3850M autoclave manufactured by Heidolph-Brinkman was used to prepare sterile solutions. The oven used to grow bacterial cell cultures was purchased from Fischer Scientific. The C76 shaking water bath was manufactured by New Brunswick Scientific. Mini-PROTEAN® TGX™ SDS-PAGE gels, the Mini-PROTEAN®II Electrophoresis cell, Power Pac 300, Precision Plus Protein™ Dual Color protein marker were purchased from Bio-Rad. Green Master Mix was purchased from Promega. Zeocin™ and YNB were purchased from Invitrogen. XhoI, XbaI and BstXI were purchased from New England Biolabs. An Avanti J-251 centrifuge manufactured by Beckman was used to pellet cell cultures. *Micrococcus lysodeiktitus*, DTT, Antifoam 204 and Sorbitol were purchased from Sigma-Aldrich. The orbital shaker used to destain gels

was purchased from Cole Parmer. The automated temperature controller-magnetic stirrer apparatus was purchased from Haake. NANOSEP 3K centrifugal filters were purchased from Pall life sciences. 250 mL and 1 L baffled flasks were purchased from Thermo-Fischer.

### ***Preparation of Yeast Vector pPICZ $\alpha$ A® for Ligation***

The plasmid pPICZ $\alpha$ A from Invitrogen was chosen as the vector for protein expression in yeast. Zeocin™ resistance is used as selective marker. This plasmid is engineered for the extra-cellular expression of the desired gene, which is induced by the presence of methanol as a source of carbon. Preparation of recombinant DNA involves the following 2 steps: (1) linearization of the pPICZ $\alpha$ A plasmid, and (2) ligation the of N103H gene into the linearized plasmid.

### ***Linearization of pPICZ $\alpha$ A plasmid***

A volume of 30  $\mu$ L of pPICZ $\alpha$ A in TOP10 *E. coli* was spread on low salt LB plates (0.5% yeast extract, 1.0% tryptone, 0.5% NaCl, 1.5% agar, pH 7.5) containing 100  $\mu$ g/mL Zeocin™. Plates were incubated overnight at 37 °C. Two colonies from the initial growth were selected and grown overnight at 37 °C in 2 mL of low salt LB medium in a shaking incubator at 225 rpm. The plasmid pPICZ $\alpha$ A was isolated using a QIA Prep® Spin Miniprep Kit. Double digestion of the plasmid was performed using two restriction enzymes, XhoI and XbaI. The reaction was as follows: 4  $\mu$ L of 50 ng/ $\mu$ L pPICZ $\alpha$ A plasmid, 2  $\mu$ L of 10 mg/mL BSA, 2  $\mu$ L of NE Buffer 4, 1  $\mu$ L of XhoI and 1  $\mu$ L of XbaI. The reaction mixture was incubated for 2 hours at 37 °C. 5  $\mu$ L of DNA was then loaded onto a 1% agarose gel and run at 85V for 52 minutes. The gel was soaked in a

solution of 5 µg/mL ethidium bromide in 1X TAE buffer for 15 minutes and visualized using an Ultra-LUM UV-Light Box.

### ***Ligation of N103H Gene into Linearized pPICZαA Plasmid***

Using the Quick Ligation protocol from New England BioLabs the N103H gene (previously prepared by Nicole Patton) was ligated into the pPICZαA plasmid. The concentration of insert (gene) and of vector were calculated by the equation

$$ng\ insert = \frac{ng\ vector \times kbp\ insert}{Kbp\ vector} * molar\ ratio \frac{insert}{vector}$$

The ligation mixture was prepared as follows: 5 µL of 10 ng/µL of N103H, 1 µL of 50 ng/µL of pPICZαA, 1 µL of Quick Ligase™, 10 µL of ligase buffer and 4 µL of sterile water. The reaction was incubated at room temperature for 5 minutes. A 2 µL volume of the above reaction was added to 50 µL of One Shot® Mach1™-T1® chemically competent *E. coli* cells and mixed gently. The tube was then incubated on ice for 30 minutes. The cells were heat shocked at 42 °C for 30 seconds and immediately transferred to ice. A 250 mL aliquot of SOC media (super optimal media with catabolite repression) was added to the tube, and the tube was incubated at 37 °C for 1 hour with horizontal shaking at 200 rpm. Different volumes ranging from 100-200 µL of the reaction mixture were plated on low-salt LB with 100 µg/mL of Zeocin™. The plates were incubated overnight at 37 °C. Four colonies that were believed to be transformed with *hewl*-N103H-pPICZαA recombinant DNA were re-streaked and incubated overnight at 37 °C. A colony was inoculated into 2 mL of low salt LB broth with 100 µg/mL Zeocin™ and grown overnight with shaking at 225 rpm at 37 °C. The recombinant DNA was isolated using the QIA prep® Spin Miniprep Kit.



### ***Confirmation of Ligation of the Mutant Genes into pPICZαA Plasmid***

A double digest was performed to confirm the ligation of the mutant gene into the pPICZαA plasmid. Double digestion was performed using the restriction enzymes XhoI and XbaI. The reaction mixture was prepared as follows: 4 μL of 50 ng/μL *hewl*-N103H-pPICZαA, 2 μL of BSA, 2 μL of NE buffer 4, 1 μL of XhoI, 1 μL of XbaI and 11 μL of sterile water were mixed in a PCR tube. The reaction mixture was incubated overnight at 37 °C. 5 μL of the reaction mixture were then heated to 65 °C for 20 minutes in order to inactivate the restriction enzymes. 5 μL of the heat inactivated reaction mixture was loaded onto a 1% agarose gel and run at 85 V for 55 minutes. The gel was soaked in a solution of 5 μg/mL ethidium bromide in 1X TAE buffer for 15 minutes and visualized using an Ultra-LUM UV-Light Box.

### ***Linearization of *hewl*-N103H-pPICZαA for Yeast Transformation***

A transformed *E. coli* colony was chosen and inoculated in 2 mL of low salt LB broth containing 100 μg/mL of Zeocin™. Cells were cultured for 8 hours at 37 °C by shaking at 225 rpm. A volume of 10 μL was distributed into 10 different tubes with 2 mL of low salt LB broth with 100 μg/mL Zeocin™ in each and shaken at 225 rpm for 12-14 hours at 37 °C. The DNA from each tube was isolated using the QIA prep® Spin Miniprep Kit and pooled into one microcentrifuge tube giving a total of about 300 μg of DNA. One-tenth volume of sodium acetate (3M, pH 5.2) was added, followed by addition of 0.7X volume of isopropanol at room temperature. The solution was centrifuged at 13,000 rpm for 30 minutes at 4 °C. The supernatant was decanted and the pellet was rinsed with 70% ethanol and centrifuged at 13,000 rpm for 15 minutes at room temperature. The supernatant was discarded. To the precipitated *hewl*-N103H-pPICZαA



DNA pellet, 5  $\mu$ L of BSA, 5  $\mu$ L of NE Buffer 4, 5  $\mu$ L of BstXI and 35  $\mu$ L of sterile water were added. The reaction mixture was incubated at 37 °C for 1.5 hours. 5  $\mu$ L of the reaction mixture was loaded onto a 1% agarose gel and run at 85 V for 55 minutes. The gel was soaked in a solution of 5  $\mu$ g/mL ethidium bromide in 1X TAE buffer for 15 minutes and visualized using an Ultra-LUM UV-Light Box.

### ***Preparation of Competent Cells***

Competent cells were prepared following the procedure in the Easy Select™ Pichia Expression Kit manual. X-33 and KM17H strains of *P. pastoris* were streaked on YPD plates (1.0% yeast extract, 2% peptone, 2% dextrose, 2% agar) plates and incubated for 3 days at 30 °C. A colony was chosen and inoculated into 10 mL of YPD broth and shaken overnight at 250 rpm at 30 °C. 100  $\mu$ L of the overnight culture was inoculated into 10 mL of fresh YPD medium and shaken overnight at 250 rpm for 16-18 hours until the OD<sub>600</sub> was 1.3-1.5 absorbance units. The cells were harvested by centrifugation at 1500  $\times$  g at 4 °C for 5 minutes. The pellet was resuspended with 500 mL of ice cold sterile water. Cells were again centrifuged at 1500  $\times$  g for 5 minutes and resuspended in 250 mL of ice cold sterile water. The cells were centrifuged at 1500  $\times$  g for 5 minutes, the supernatant was discarded, and 20 mL of ice cold 1 M sorbitol were added. The cells were again centrifuged at 1500  $\times$  g for 5 minutes. The pellet was resuspended in 1 mL of ice cold 1 M sorbitol and kept on ice before electroporation.

### ***Transformation of Yeast***

10  $\mu$ L of 100  $\mu$ g/ $\mu$ L linearized recombinant *hewl*-N103H-pPICZ $\alpha$ A were mixed with 80  $\mu$ L of X-33 or KM17H competent cells. The mixture was transferred into an ice cold 2 mm electroporation cuvette and incubated on ice for 5 minutes. The cells were

then pulsed at 1.5 kV, 25  $\mu$ F and 186  $\Omega$ . After pulsing, the cells were then washed immediately with 1 mL of 1 M ice cold sorbitol and the contents were transferred to a 15 mL sterile tube. The tube was then incubated for 1.5 hours at 30 °C. Volumes of 50  $\mu$ L, 100  $\mu$ L, 150  $\mu$ L and 200  $\mu$ L were spread on YPDS plates (1.0% yeast extract, 2% peptone, 2% dextrose, 2% agar, 1M sorbitol) containing 100  $\mu$ g/mL Zeocin™. The plates were incubated at 30 °C for at least 3 days. Four colonies that grew were re-streaked on YPD plates with 100  $\mu$ g/mL Zeocin™ and incubated for at least 3 days at 30 °C.

### ***Confirmation of Yeast Transformation by the Polymerase Chain Reaction***

A PCR analysis was performed to confirm the integration of the *hewl*-N103H-pPICZ $\alpha$ A plasmid into the yeast genome. A 1.5 mL culture of transformed yeast was grown in YPD broth with 100  $\mu$ g/mL Zeocin™ overnight at 30 °C at 225 rpm. The cells were harvested by centrifugation at 13,000 rpm for 3 minutes and the supernatant was discarded. 200  $\mu$ L of Harju Buffer was added (2% Triton X-100, 1 % SDS, 100 mM NaCl, 10 mM Tris-HCl pH 8.0, and 1 mM EDTA). The tubes were immersed in a dry ice/ethanol bath for 2 minutes. The tubes were then transferred immediately to a heat block which was set at 95 °C for 1 minute. This freeze-thaw cycle was repeated 2 more times and the tubes were vortexed for 30 seconds. After vortexing, the tubes then were centrifuged at 13,000 rpm for 3 minutes at room temperature. The aqueous layer (upper layer) was transferred to a new tube with 400  $\mu$ L of ice cold 100% ethanol. The tube was then mixed by inversion 5-10 times and then incubated for 10 minutes at -20 °C. The tubes were centrifuged at 13,000 rpm for 5 minutes at room temperature and the supernatant was removed. The pellet was washed with 500  $\mu$ L of 70% ethanol at room temperature, and the tubes were centrifuged at 13,000 rpm for 5 minutes at room

temperature. The supernatant was removed and the pellet was dried at room temperature for 15 minutes. The pellet was resuspended in 30  $\mu$ L of 1X TE buffer (10 mM Tris, 1 mM EDTA, pH 8.0). RNase treatment was performed to remove unwanted RNA by adding 1  $\mu$ L of 10  $\mu$ g/mL RNase and the tube was incubated at 37  $^{\circ}$ C for 30 minutes. One-tenth volume of 3M CH<sub>3</sub>COONa (pH 6.8) and 2 times the volume of 95% ethanol were added and the mixture was incubated on ice for 10 minutes. The tube was then centrifuged at 13,000 rpm for 5 minutes and the supernatant was removed. The pellet was washed again with 10  $\mu$ L of 70% ethanol and was dried at 37  $^{\circ}$ C for 30 minutes. The DNA was dissolved in 30  $\mu$ L of 1X TE buffer. A 5  $\mu$ L volume of DNA was loaded onto a 1% agarose gel and run at 85 V for 55 minutes. The gel was soaked in a solution of 5  $\mu$ g/mL ethidium bromide in 1X TAE buffer for 15 minutes and visualized using an Ultra-LUM UV-light box.

The PCR sample was prepared as follows: 10  $\mu$ L of Promega Master Mix™, 2 $\mu$ L of 5' *AOX1* primer (10  $\mu$ M), 2 $\mu$ L of 3' *AOX1* primer (10  $\mu$ M), 5  $\mu$ L of yeast DNA and 1 mL of nuclease free water were mixed in a PCR tube. The Technegene (version 10.19) thermocycler was used to perform the PCR reaction. The program consisted of the following steps: initial denaturation at 94  $^{\circ}$ C for 3 min, then a loop repeated for 30 times consisting of heat denaturation at 94  $^{\circ}$ C for 1 min, annealing at 55  $^{\circ}$ C for 1 min and an extension at 72  $^{\circ}$ C for 1 min. At the end of 30 cycles a final extension step at 72  $^{\circ}$ C for 10 minutes was performed. A 5  $\mu$ L volume of the PCR product was loaded onto a 1% agarose gel and run at 85 V for 55 minutes. The gel was soaked in a solution of 5  $\mu$ g/mL ethidium bromide in 1X TAE buffer for 15 minutes and visualized using an Ultra-LUM UV-light box.

### ***Expression of Mutant Proteins***

A 1.5 mL culture of transformed X-33 yeast colonies 1 and 4 were grown overnight at 30 °C at 225 rpm in YPD media. 10 µL of the overnight culture was inoculated into 25 mL of buffered glycerol medium (BMGY, 1% yeast extract, 2% peptone, 1.34% YNB,  $4 \times 10^{-5}$ % biotin, 1% glycerol, 100 mM potassium phosphate, pH 6.0) in a 250 mL baffled flask. The culture was grown at 30 °C in a shaking water bath for 16-18 hours until the OD<sub>600</sub> reached 2-6 absorbance units. The cells were then harvested by centrifugation at  $3000 \times g$  for 5 minutes at room temperature. The cells were then suspended to an OD<sub>600</sub> of 1.0 in 100 mL of buffered minimal methanol medium BMMY (1% yeast extract, 2% peptone, 1.34% YNB,  $4 \times 10^{-5}$ % biotin, 0.5% methanol, 100 mM potassium phosphate, pH 6.0) medium to induce expression. The culture was placed in a 1 liter baffled flask, covered with 2 layers of sterile cheese cloth and incubated in a shaking water bath at 30 °C at 225 rpm for 4 days. 100 % methanol was added every 24 hours to the growth media to a final concentration of 0.5% methanol. At each of the time points 0, 6, 12, 24, 36, 48, 60, 72, 84, 96 hours 1 mL of the expression culture was transferred to a microcentrifuge tube and centrifuged at 13,000 rpm for 3 minutes at room temperature. The supernatant was transferred to a separate tube. The supernatant and cell pellets were stored at -80 °C. GS115/Mut<sup>r</sup> and pPICZαA in X-33 strain of *Pichia pastoris* were grown as controls.

An identical protocol was followed using transformed X-33 under the following conditions: (1) BMMY at pH 6.0 with 0.005% antifoam 204 and biotin prepared using 0.05M NaOH, (2) BMMY at pH 7.0 with 0.005% antifoam 204 and biotin prepared using 0.05M NaOH and (3) initial growth in unbuffered minimal glycerol medium MGH

(1.34% YNB,  $4 \times 10^{-5}$ % biotin dissolved in 0.05M NaOH, 1% glycerol) and a second growth using unbuffered minimal methanol medium, MMH (1.34% YNB,  $4 \times 10^{-5}$ % biotin dissolved in 0.05M NaOH, 1% methanol). 100 % methanol was added every 24 hours to the growth media to a final concentration of 0.5% methanol. At each of the time points 0, 6, 12, 24, 36, 48, 60, 72, 84, 96 hours 1 mL of the expression culture was transferred to a microcentrifuge tube and centrifuged at 13,000 rpm for 3 minutes at room temperature. The supernatant was transferred to a separate tube. Both the cell pellet and the supernatant were stored at  $-80^{\circ}\text{C}$ .

### *Analysis of Mutant Proteins*

#### *SDS-PAGE*

Mini-PROTEAN<sup>®</sup> TGX<sup>™</sup> Precast gels with a 4-20% resolving gel from Bio-Rad were used to analyze the supernatant fractions by SDS-PAGE. 20  $\mu\text{L}$  of supernatant was mixed with 20  $\mu\text{L}$  of 2X protein loading dye from Amresco. The sample was heated at  $95^{\circ}\text{C}$  for 3 minutes and centrifuged for 30 seconds at 13,000 rpm. A volume of 20  $\mu\text{L}$  was loaded into each well. 10  $\mu\text{L}$  of Precision Plus Protein<sup>™</sup> Dual Color protein marker (250kD-10kD) was loaded in one well. The gel was run at 180 V for about 75 minutes until the tracking dye reached the bottom of the gel. The gel was removed and placed in a Tupperware container filled with 25 mL DDI water and microwaved for 1 minute. This process was repeated 2 more times with fresh DDI water. 25 mL of Blue BANDit<sup>™</sup> protein stain was added and the gel was microwaved for 1 minute. The gel was shaken for 15 minutes at 75 rpm in an orbital shaker and the dye was decanted. The gel was destained by adding 25 mL DDI water and shaken for 30 minutes. Kimwipes<sup>™</sup> were placed in the container to facilitate the removal of protein dye. The water was then

decanted and replaced with fresh water and Kimwipes™ and allowed to destain overnight on an orbital shaker set to 75 rpm.

### ***Bradford Assay***

Samples for the Bradford assay were prepared according to Table 2.1. The prepared samples were vortexed for 5 seconds and then incubated for 10 min at room temperature. The absorbance at 595 was measured and recorded.

Table 2.1: Preparation of samples for the Bradford assay.

Sample	Test Tube					
	Blank	Std. 1	Std. 2	Std. 3	Std. 4	Supernatant samples
BSA std(μL)	0	10	30	50	70	0
Water(μL)	100	90	70	50	30	0
Supernatant (μL)	0	0	0	0	0	100
Coomassie reagent (mL)	3	3	3	3	3	3

### ***Enzyme Assay***

The supernatant was assayed for lysozyme activity by visible spectroscopy.<sup>22</sup> A suspension of *Micrococcus lysodeikticus* (0.3 mg/mL) was prepared by suspending 15 mg of cells in 50 mL of 0.1 M potassium phosphate buffer at pH 7.0. The cells were incubated in buffer for 24 hours at 4 °C to hydrate the cells prior to performing the assays. Ultra-Pure HEWL purchased from Amresco was assayed as a control. 2.9 mL of *Micrococcus lysodeikticus* cell suspension and three, 2 mm magnetic stir bars were added to a glass cuvette and placed in a cuvette holder attached to a circulating water bath to maintain the temperature. The cell suspension was allowed to equilibrate to 25 °C for 5 minutes. 100 μL of diluted lysozyme standard was added to the cuvette and the decrease

in absorbance was observed at 450 nm for 2.5 minutes. The control was further diluted until the  $\Delta A_{450}/\text{min}$  was between 0.0150-0.0400 range. 100  $\mu\text{L}$  of supernatant were used in place of the native enzyme to measure the activity of the expressed protein.

## CHAPTER 3: RESULTS

### *Preparation of Yeast Vector pPICZ $\alpha$ A<sup>®</sup> for Ligation*

The pPICZ $\alpha$ A plasmid DNA in TOP10 *E. coli* was isolated in order to prepare recombinant DNA with the N103H mutant HEWL gene. Figure 3.1 shows the isolated pPICZ $\alpha$ A plasmid DNA. Lane 1 is the 100 bp DNA ladder, lanes 3, 4, 5 and 6 shows the isolated pPICZ $\alpha$ A DNA and lane 8 shows the 1 kbp DNA ladder.

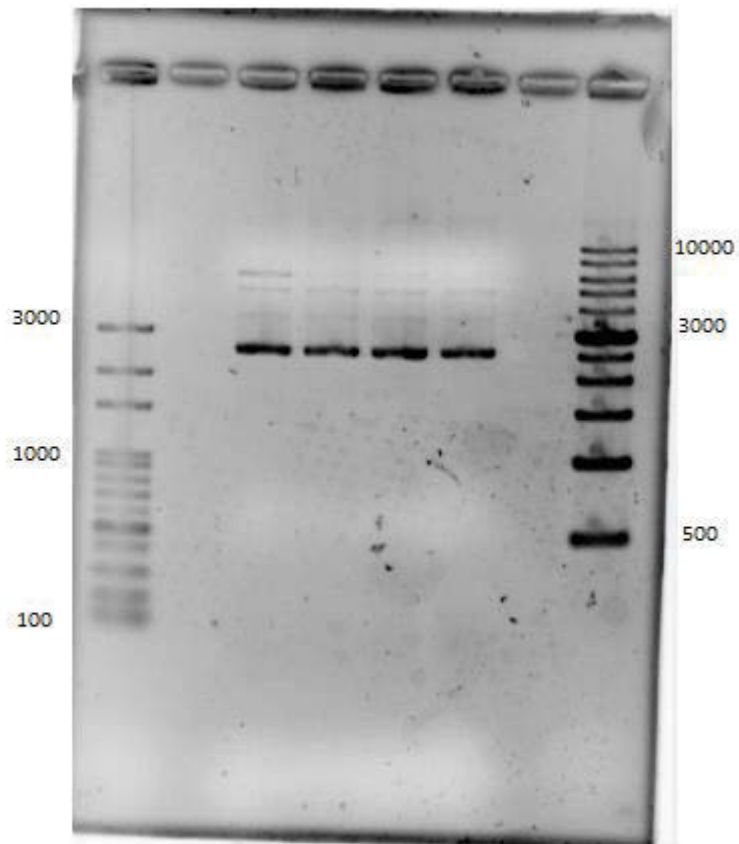


Figure 3.1: A gel image of isolated pPICZ $\alpha$ A plasmid DNA. Lane 1: 100 bp DNA ladder, Lane 3-6: pPICZ $\alpha$ A plasmid DNA, Lane 8: 1 kbp DNA ladder.

### *Linearization of the pPICZ $\alpha$ A Plasmid*

Isolation of pPICZ $\alpha$ A plasmid was followed by its linearization using restriction enzymes XhoI and XbaI. In Figure 3.2, Lane 1 shows the 100 bp DNA ladder, lanes 3



and 5 shows the digested pPICZ $\alpha$ A DNA and lane 8 shows the 1 kbp DNA ladder. The pPICZ $\alpha$ A plasmid band is seen between 4 kbp and 3 kbp as the pPICZ $\alpha$ A plasmid is approximately 3.6 kbp long.

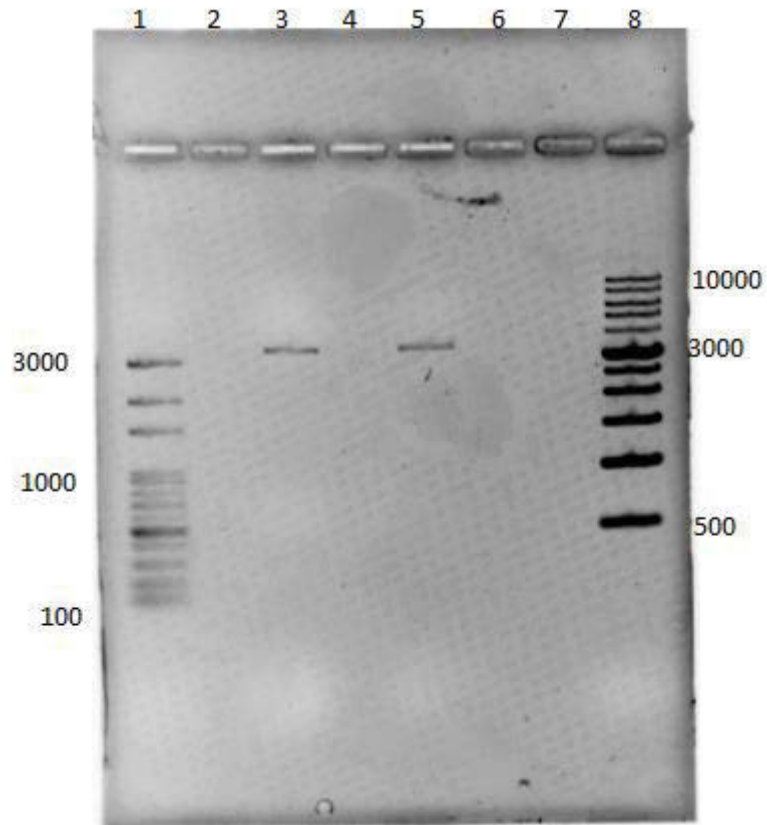


Figure 3.2: A gel image of linearized pPICZ $\alpha$ A plasmid DNA. Lane 1: 100 bp DNA ladder, Lane 3 and 5: linearized pPICZ $\alpha$ A plasmid DNA, Lane 8: 1 kbp DNA ladder.

### ***Ligation of the N103H gene into the Linearized pPICZ $\alpha$ A Plasmid***

The mutant N103H gene was ligated into linearized pPICZ $\alpha$ A plasmid. Growth of transformed One Shot<sup>®</sup> Mach1<sup>™</sup>-T1<sup>®</sup> *E.coli* colonies on low salt LB plates with 100  $\mu$ g/mL Zeocin<sup>™</sup> indicated that the ligation reaction was successful. Figure 3.3 shows a gel of the DNA isolated from the transformed bacteria after the ligation reaction. A single band near 4 kbp indicated that the pPICZ $\alpha$ A plasmid had been successfully ligated with

the N103H mutant HEWL gene. Lane 1 corresponds to the 100 bp DNA ladder, lane 6 corresponds to *hewl*-N103H-pPICZ $\alpha$ A plasmid and lane 8 corresponds to 1 kbp DNA ladder.

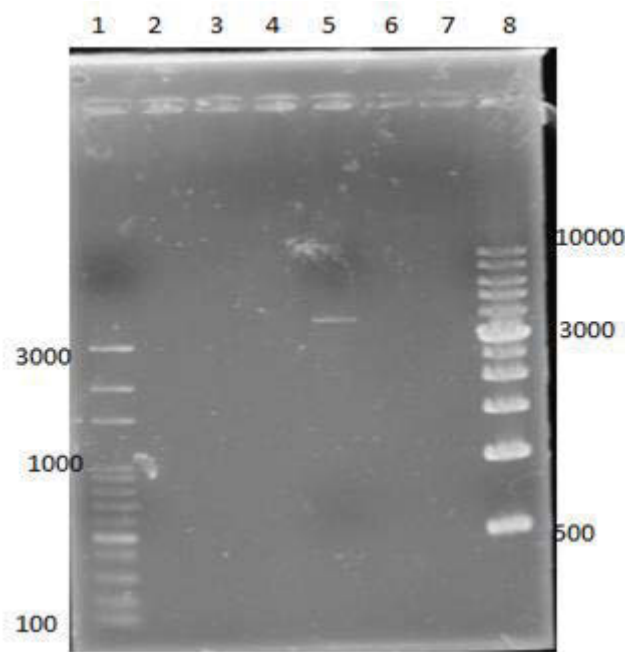


Figure 3.3: A gel image of ligated *hewl*-N103H-pPICZ $\alpha$ A plasmid DNA, Lane 1: 100 bp DNA ladder, Lane 5: *hewl*-N103H-pPICZ $\alpha$ A plasmid DNA, Lane 8: 1 kbp DNA ladder.

#### ***Confirmation of Ligation Reaction:***

A double digest with XhoI and XbaI restriction enzymes followed by agarose gel electrophoresis was performed to confirm the ligation reaction. Figure 3.4 shows an agarose gel of the double digested *hewl*-N103H-pPICZ $\alpha$ A plasmid. Lane 1 and Lane 8 corresponds to 100 bp and 1 kbp DNA ladders respectively. Lane 4 corresponds to a DNA sample digested with the two restriction enzymes XhoI and XbaI in which two bands are observed at 3.6 kbp and 400 bp which corresponds to the size of the pPICZ $\alpha$ A plasmid and the mutant gene respectively. Lane 5 corresponds to a digestion mixture using just one restriction enzyme, XhoI, and Lane 6 corresponds to a digestion mixture

with just XbaI. These two served as controls to ensure that the both restriction enzymes had activity.

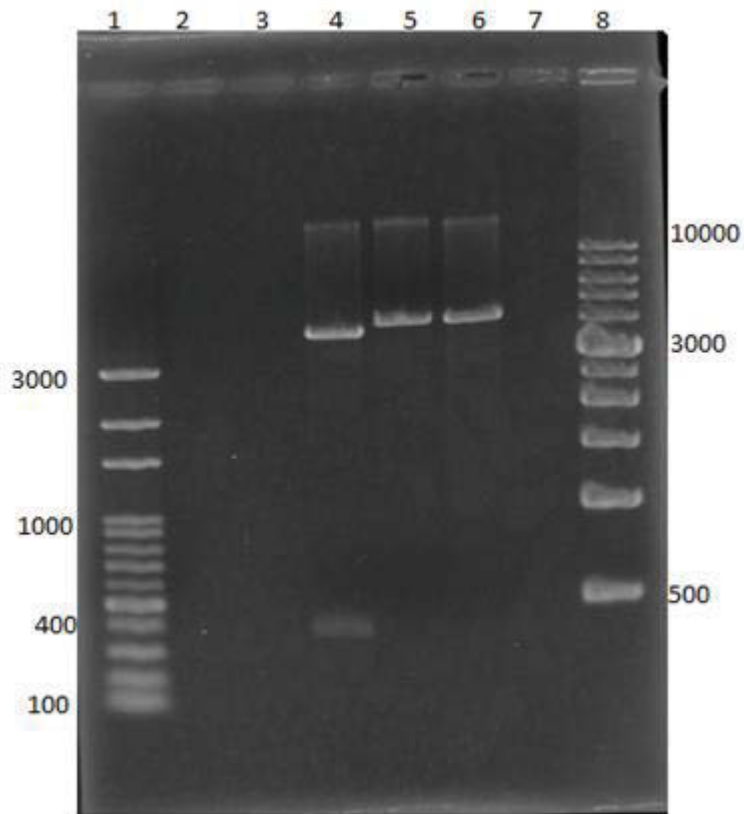


Figure 3.4: A gel image of double digest of *hewl-N103H-pPICZ $\alpha$ A* plasmid DNA. Lane 1: 100 bp DNA ladder, Lane 4: *hewl-N103H-pPICZ $\alpha$ A* plasmid DNA treated with both restriction enzymes XhoI and XbaI, Lane 5: *hewl-N103H-pPICZ $\alpha$ A* plasmid DNA treated with XhoI only, Lane 6: *hewl-N103H-pPICZ $\alpha$ A* plasmid DNA treated with XbaI only, Lane 8: 1 kbp DNA ladder.

#### ***Linearization of hewl-N103H-pPICZ $\alpha$ A for Yeast Transformation***

The linearization reaction was performed using BstXI. The digest was examined by agarose gel electrophoresis. A single band at 4 kbp indicated that pPICZ $\alpha$ A plasmid containing the mutant gene was linearized. In Figure 3.5 Lane 4 and Lane 8 corresponds to 100 bp and 1 kbp DNA ladders respectively. Lane 6 corresponds to linearized DNA. The band corresponds to 4000 bp - the expected size of the recombinant DNA.

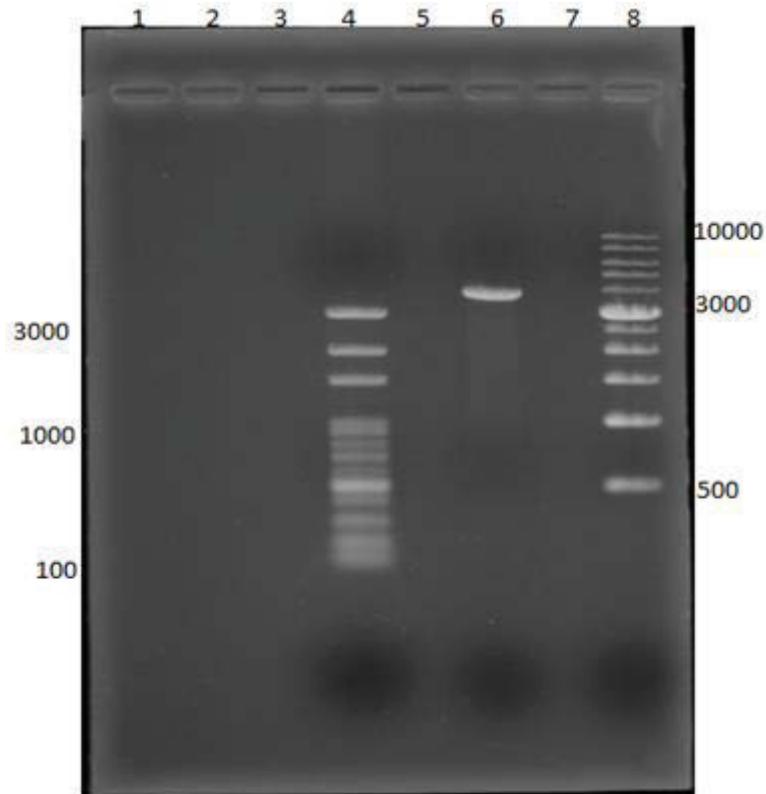


Figure 3.5: A gel image of linearized *hewl*-N103H-pPICZ $\alpha$ A plasmid DNA. Lane 4: 100 bp DNA ladder, Lane 6: *hewl*-N103H-pPICZ $\alpha$ A plasmid DNA treated with BstXI restriction enzyme, Lane 8: 1 kbp DNA ladder.

#### ***Preparation of Competent Pichia pastoris Cells***

X-33 and KM17H strains of *Pichia pastoris* were made competent for electroporation. Figure 3.6A and Figure 3.6B show X-33 and KM17H strains respectively prior to preparation of competent cells.

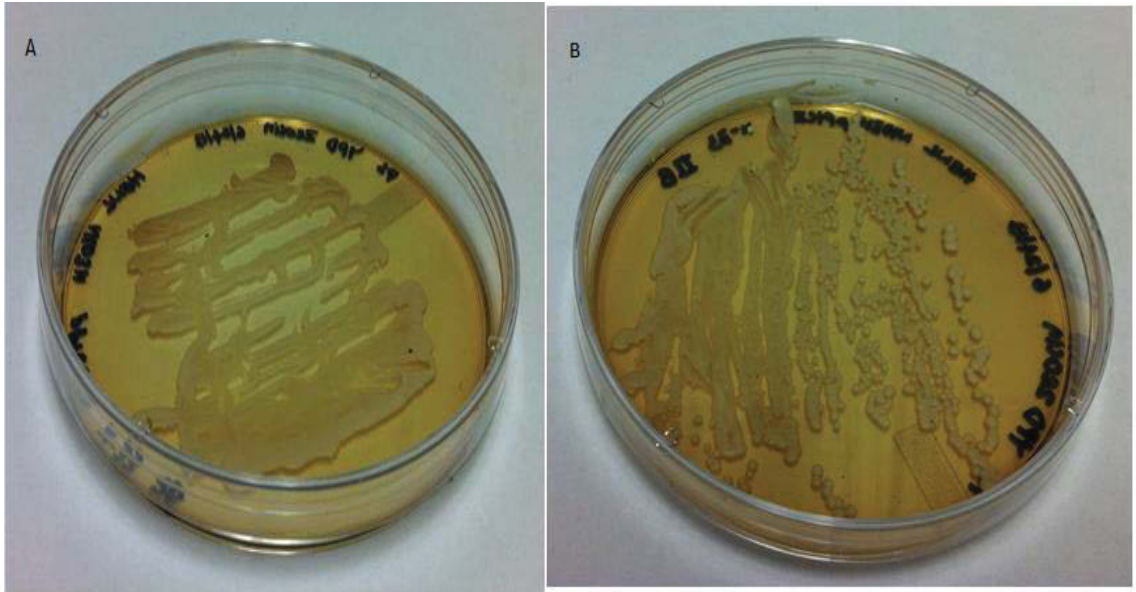


Figure 3.6: A picture of the two strains of *P. pastoris* used for electroporation: (A) X-33 (B) KM71H on YPD plates.

***Growth of Yeast after Electroporation:***

After electroporation, different volumes (50  $\mu$ L, 100  $\mu$ L, 150  $\mu$ L, 200  $\mu$ L) of cells were spread on YPDS plates (1% yeast extract, 2% peptone, 2% dextrose, 1M sorbitol, and 2% agar) containing 100  $\mu$ g/mL of Zeocin<sup>TM</sup>. Figure 3.7 A and B shows the transformed colonies that were selectively grown on YPDS plates with Zeocin<sup>TM</sup>. Four colonies were re-streaked on YPD plates containing 100  $\mu$ g/mL Zeocin<sup>TM</sup>. Figure 3.8 A through D show the transformed yeast colonies on YPD with Zeocin<sup>TM</sup> plates. Electroporation with the KM17H strain of yeast was not successful.

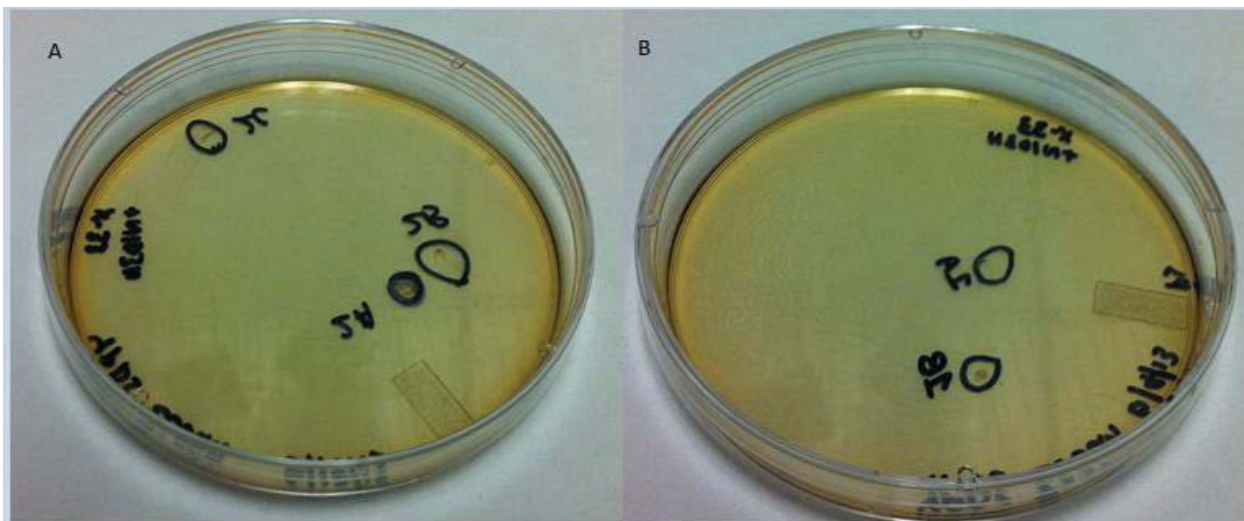


Figure 3.7: (A) Picture of transformed X-33 with *hewl*-N103H-pPICZ $\alpha$ A after electroporation. Three colonies were selected that grew on the 200  $\mu$ L volume plates (colonies 1, 2 and 3); (B) Picture of transformed X-33 with *hewl*-N103H-pPICZ $\alpha$ A after electroporation, two colonies were marked that grew with a volume 150  $\mu$ L plated (colonies 4 and 5).

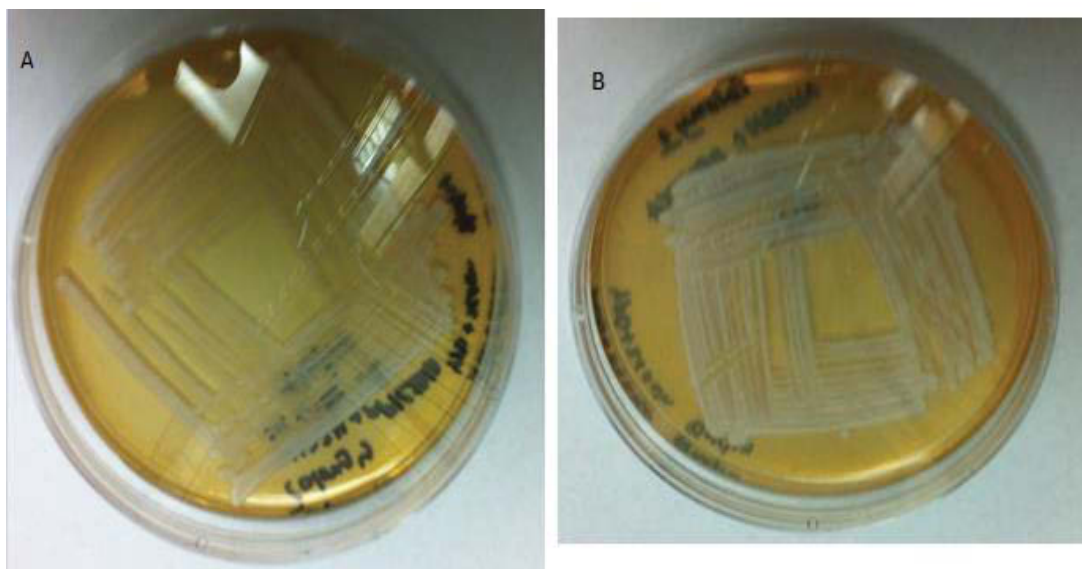


Figure 3.8: (A) Picture of transformed X-33 with *hewl*-N103H-pPICZ $\alpha$ A re-streaked on YPD plates with Zeocin<sup>TM</sup> (colony 1). (B) Picture of transformed X-33 with *hewl*-N103H-pPICZ $\alpha$ A re-streaked on YPD plates with Zeocin (Colony 2).



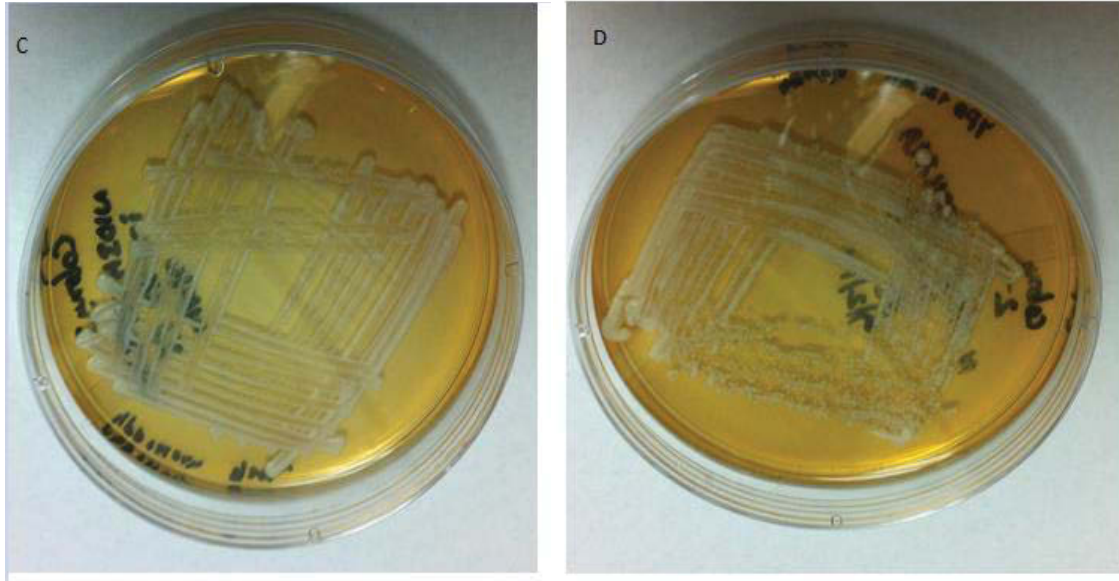


Figure 3.8: (C) Picture of transformed X-33 with *hewl*-N103H-pPICZ $\alpha$ A re-streaked on YPD plates with Zeocin<sup>TM</sup> (colony 3). (D) Picture of transformed X-33 with *hewl*-N103H-pPICZ $\alpha$ A re-streaked on YPD plates with Zeocin<sup>TM</sup> (colony 4).

#### ***Confirmation of Yeast Transformation by the Polymerase Chain Reaction***

PCR analysis was performed to verify the intergation of the gene into the *Pichia* genome and also to determine the mutant phenotype. Yeast genomic DNA was isolated using Harju Buffer. A 1% agarose gel showed a very high molecular weight band of DNA corresponding to genomic yeast DNA (Figure 3.9). In Figure 3.10 the control shows a band near 1 kbp as the primers amplify a nearly 600 bp region of pPICZ $\alpha$ A as well as the 400 bp gene. A band at about 2 kbp corresponds to the *AOX1* gene which is approximately 2.2 kbp in length. This clearly indicates that the *Pichia* clones are Mut<sup>+</sup> integrants.

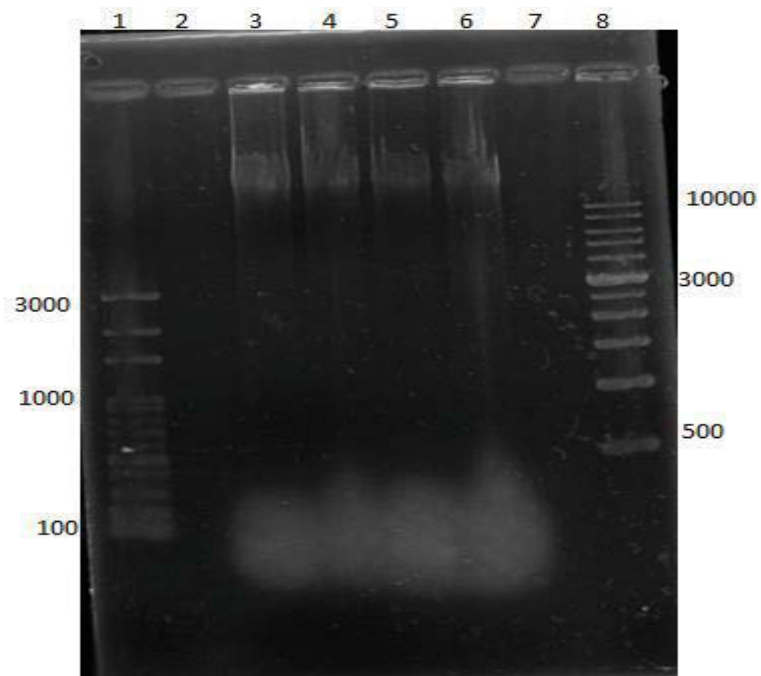


Figure 3.9: A gel image of genomic DNA isolated from transformed X-33 yeast. Lane 1: 100 bp DNA ladder, Lane 3-6: genomic DNA of yeast colonies 1-4 respectively, Lane 8: 1 kbp DNA ladder.

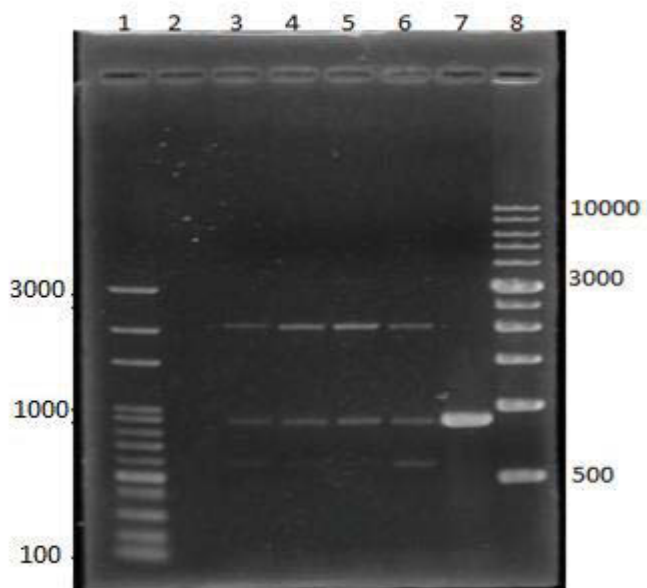


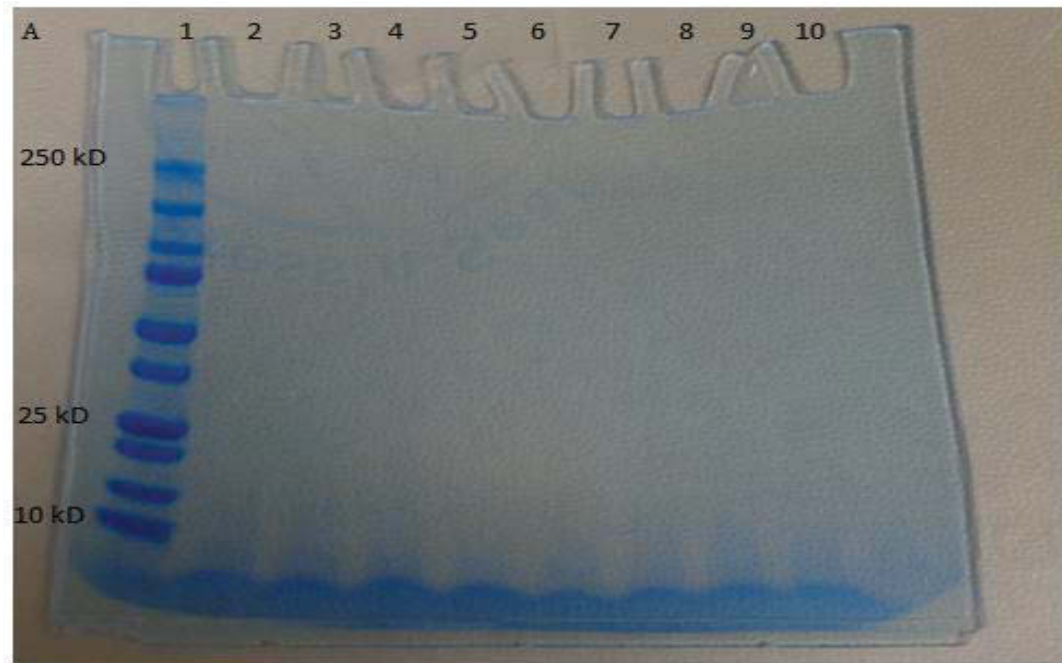
Figure 3.10: A gel image of the PCR analysis of X-33 transformed yeast DNA. Lane 1: 100 bp DNA ladder, Lane 3-6: PCR products of transformed yeast DNA of colonies 1-4 respectively, Lane 7: Control (*hewl*-N103H-pPICZ $\alpha$ A) Lane 8: 1 kbp DNA ladder.



## *Analysis of Mutant Proteins*

### *SDS-PAGE*

SDS polyacrylamide gel electrophoresis was performed on the isolated supernatants collected over 96 hours. In Figure 3.11A and B, Lane 1 corresponds to the protein marker and the rest of the lanes correspond to the protein bands at 12 hr time intervals. The media used for this growth was a BMMY with biotin prepared in sterile water and without antifoam.



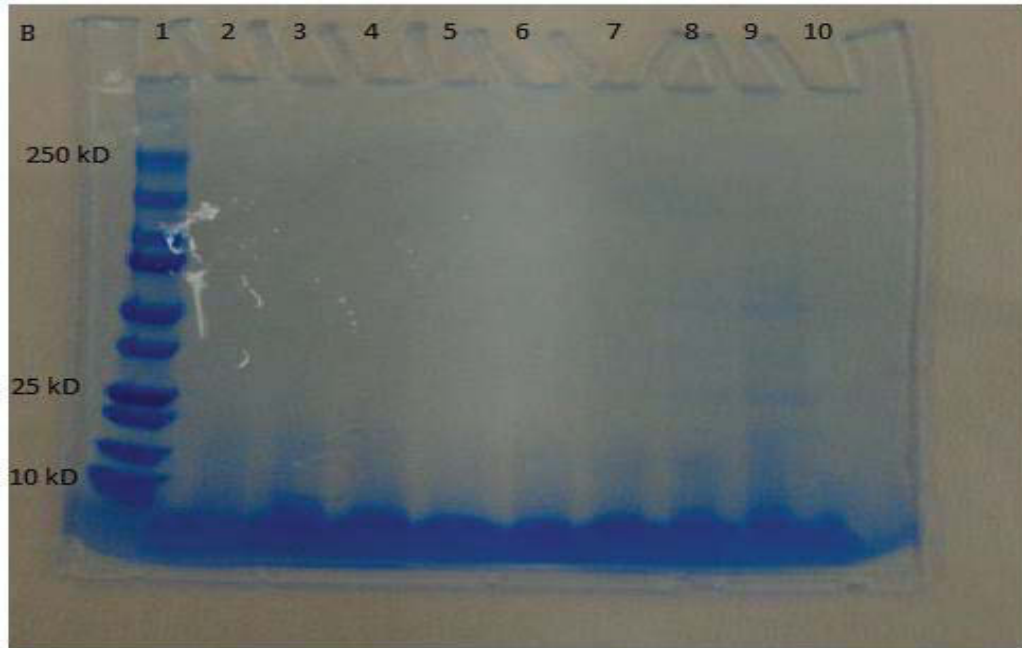


Figure 3.11: (A) An SDS-PAGE of supernatant BMMY (with biotin in water) samples of colony 1 at different time points. Lane 1 corresponds to protein marker; lane 2-10 corresponds to samples at the following time points: 12, 24, 36, 48, 60, 72, 84 and 96 hours respectively. (B) An SDS-PAGE of supernatant BMMY samples of colony 4 at different time points, lane 1 corresponds to protein marker, Lane 2-10 corresponds to samples at the following time points: 6, 12, 24, 36, 48, 60, 72, 84 and 96 hours.

A subsequent experiment was performed using the same protocol with slight modifications in the preparation of media. The media used for small scale expression contained biotin prepared in 0.05 M NaOH. Antifoam 204 was added to a concentration of 0.005% (v/v) in BMMY growth media. Figure 3.12 A shows a gel of supernatant samples at 24 hour time intervals at pH 6.0, and Figure 3.12 B shows a gel of supernatant samples at 24 hour time intervals at pH 7.0.

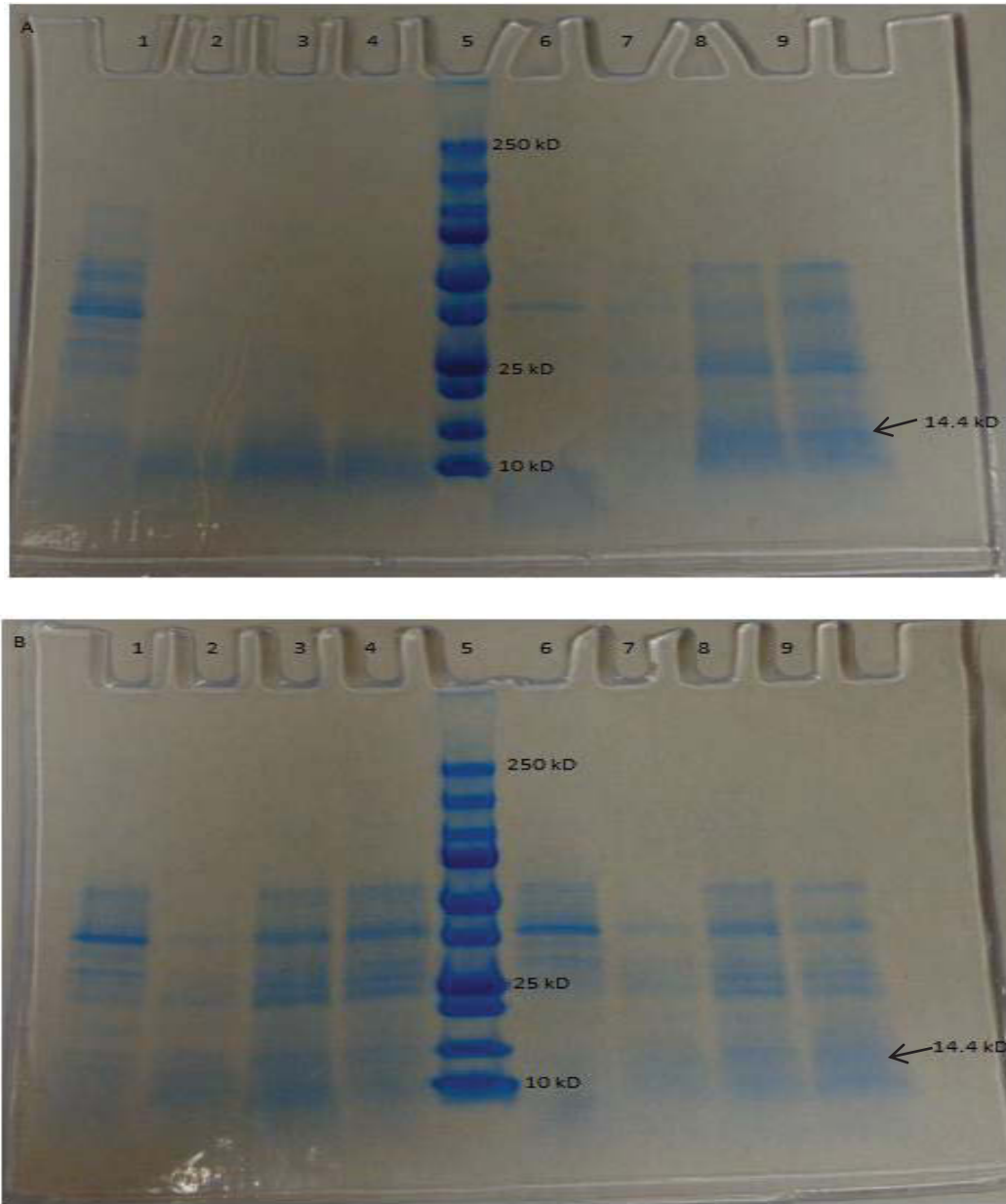


Figure 3.12: (A) An SDS-PAGE of supernatant BMMY(with Biotin in 0.05M NaOH, with antifoam) samples of colony 1 and colony 4 at pH 6.0. Lane 1-4 corresponds to samples at 24, 48, 72 and 96 hour time points of colony 1 at pH 6.0, lane 5 corresponds to protein marker, lane 4-9 corresponds to samples at 24, 48, 72 and 96 hour time points of colony 4 at pH 6.0 respectively. (B) An SDS-PAGE of supernatant BMMY(with Biotin in 0.05M NaOH, with antifoam) samples of colony 1 and colony 4 at pH 7.0. Lane 1-4 corresponds to 24, 48, 72 and 96 hour time points of colony 1 at pH 6.0, lane 5 corresponds to protein marker, lane 4-9 corresponds to samples at 24, 48, 72 and 96 hour time points of colony 4 at pH 6.0 respectively.

The molecular weight of the mutant protein in supernatant was calculated using the  $R_f$  values calculated from the gel (Table 3.1). A linear plot was drawn and the molecular weight was calculated for the band that most closely corresponds to the size of the N103H HEWL (Figure 3.13).

Table 3.1: Calculation of  $R_f$  values for each gel:

Band (kD)	$R_f$ value for gel (Fig. 3.12 A)	$R_f$ value for gel (Fig. 3.12B)
250	0.014	0.167
150	0.231	0.242
100	0.308	0.349
75	0.369	0.394
50	0.478	0.5
37	0.523	0.545
25	0.646	0.667
20	0.677	0.712
15	0.754	0.773
10	0.831	0.848
Sample	0.738	0.75

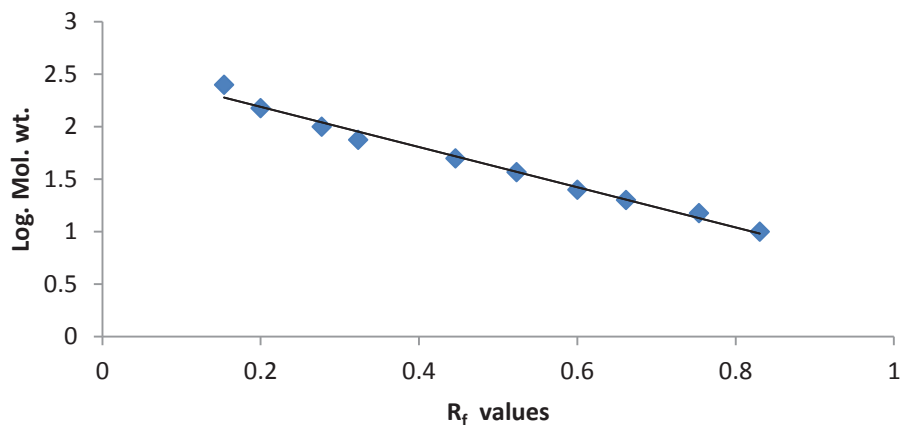


Figure 3.13: A plot of log molecular weight of the standards versus  $R_f$  values used to determine the molecular of the expressed protein.

GS115/Mut<sup>-</sup> and pPICZαA in the X-33 strain of *P. pastoris* were grown as controls at pH 6.0 and without antifoam.

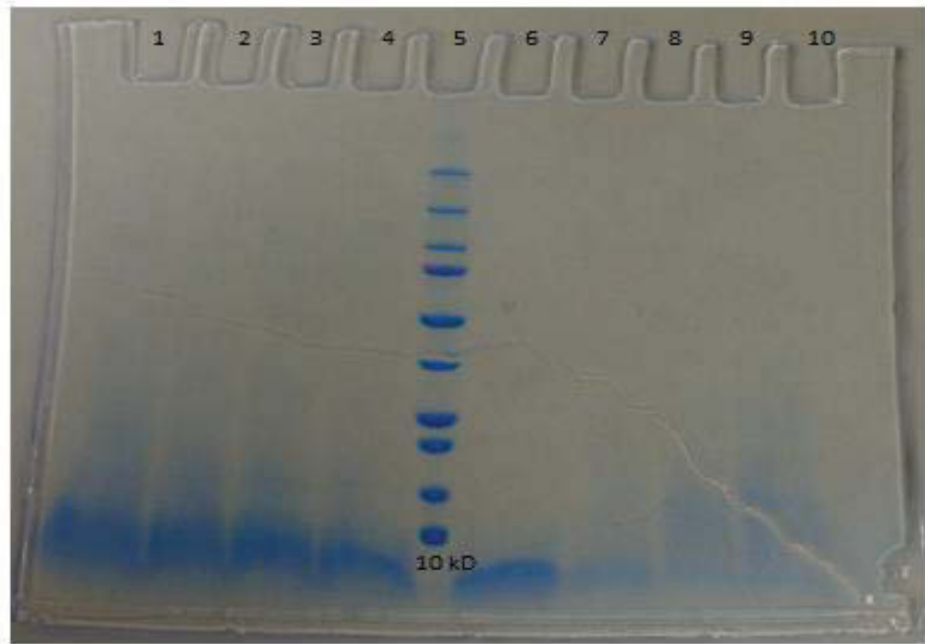


Figure 3.14: An SDS-PAGE of supernatant BMMY samples of controls (GS115/Mut<sup>-</sup> and pPICZαA in *P. pastoris*). Lane 1-4 corresponds to samples at 24, 48, 72, 96 hour time points of GS115/Mut<sup>-</sup>, lane 5 corresponds to protein marker, lane 4-9 corresponds to samples at 24, 48, 72, 96 hour time points of pPICZαA in *P. pastoris* respectively.



Figure 3.15: (A) An SDS-PAGE of supernatant samples of unbuffered MMY media (with biotin in 0.05M NaOH, with antifoam) samples of colony 1 and colony 4. Lane 1-4 corresponds to samples at 24, 48, 72, 96 hour time points of colony 1, lane 5 corresponds to protein marker, lane 6-9 corresponds to samples at 24, 48, 72, 96 hour time points of colony 4 respectively. (B) An SDS-PAGE of supernatant samples of unbuffered media MMY (with Biotin in 0.05M NaOH, with antifoam) samples of GS115/Mut<sup>-</sup> and pPICZαA in X-33 strain of *P. pastoris*. Lane 1-4 corresponds to 24, 48, 72, 96 hour time points of GS115/Mut<sup>-</sup>, lane 5 corresponds to protein marker, lane 6-9 corresponds to samples at 24, 48, 72, 96 hour time points of colony pPICZαA in X-33 strain of *P. pastoris* respectively.

**Bradford Assay:**

The Bradford assay was performed to determine the concentration of protein in the supernatant fractions. Bovine serum albumin (BSA) was used to prepare the standard curve, in which the absorbance at 595 nm of known concentrations of BSA in the dye is plotted versus the  $\mu\text{g}$  of BSA in the assay mix. Before measuring the protein concentration the 24, 48, 72, and 96 hr supernatant fractions were pooled and concentrated to about 250  $\mu\text{L}$ . The concentrate was washed with about 200  $\mu\text{L}$  of potassium phosphate buffer at pH 7.0 for two times and analyzed. A plot of the absorbance of each sample at 595 nm vs. the  $\mu\text{g}$  of BSA was prepared (Figure 3.16) and used to determine the concentration of the pooled fractions.

Table 3.2: Bradford Assay of pooled 24 hr samples.

Sample	Absorbance(595 nm)
BSA(10 $\mu\text{g}$ )	0.22347
BSA(30 $\mu\text{g}$ )	0.55973
BSA(50 $\mu\text{g}$ )	0.83468
BSA(70 $\mu\text{g}$ )	1.13090
Colony 1 , pooled 24hr samples, pH 6.0	0.14308
Colony 4 , pooled 24hr samples, pH 6.0	0.24233
Colony 1 , pooled 24hr samples, pH 7.0	0.21194
Colony 4 , pooled 24hr samples, pH 7.0	0.30157

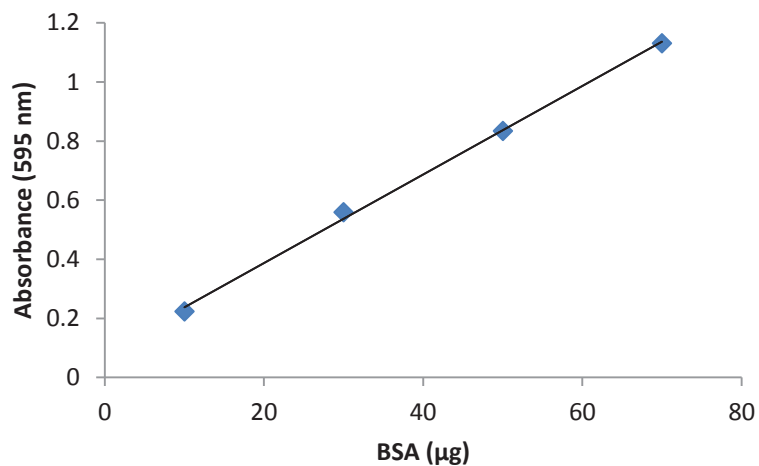


Figure 3.16: A plot of absorbance (595 nm) vs concentration of BSA ( $\mu\text{g}$ )

Table 3.3: Calculated concentration of the pooled 24 hr samples by Bradford Assay

Samples	Concentration(mg/mL)
Colony 1 , pooled 24hr samples, pH 6.0	0.0898
Colony 4 , pooled 24hr samples, pH 6.0	0.0913
Colony 1 , pooled 24hr samples, pH 7.0	0.0908
Colony 4 , pooled 24hr samples, pH 7.0	0.0922

All supernatant fractions were pooled and concentrated to about 250  $\mu\text{L}$ . The concentrate was washed with about 200  $\mu\text{L}$  of potassium phosphate buffer at pH 7.0 before being analyzed.



Table 3.4: Bradford Assay of pooled samples.

Sample	Absorbance(595 nm)
BSA(10 $\mu\text{g}$ )	0.22069
BSA(30 $\mu\text{g}$ )	0.51289
BSA(50 $\mu\text{g}$ )	0.79949
BSA(70 $\mu\text{g}$ )	1.04230
Colony 1, pooled samples, pH 6.0	0.13637
Colony 4, pooled samples, pH 6.0	0.30264
Colony 1, pooled samples, pH 7.0	0.21540
Colony 4, pooled samples, pH 7.0	0.30410

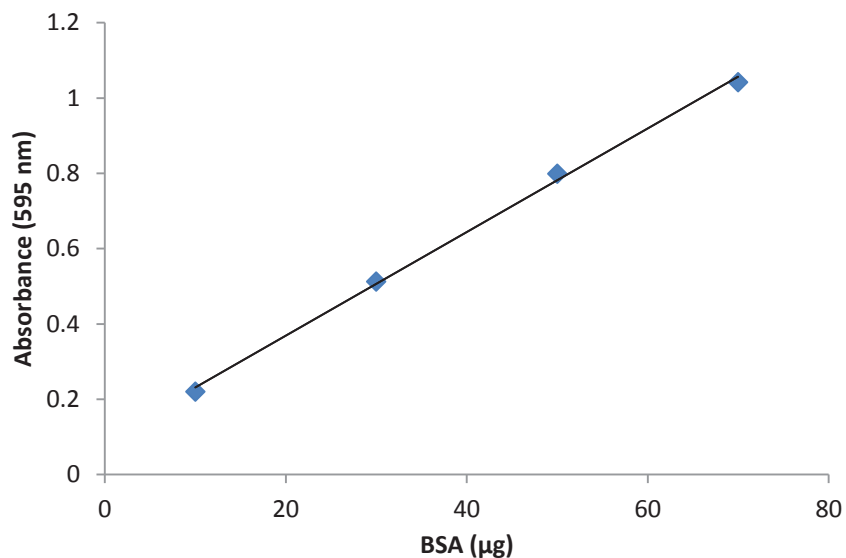


Figure 3.17: A plot of absorbance (595 nm) vs concentration of BSA ( $\mu\text{g}$ )

Table 3.5: Calculated concentration of the pooled samples by Bradford Assay

Samples	Concentration(mg/mL)
Colony 1, pooled samples, pH 6.0	0.0954
Colony 4, pooled samples, pH 6.0	0.1032
Colony 1, pooled samples, pH 7.0	0.1004
Colony 4, pooled samples, pH 7.0	0.1032

**Enzyme Assay:**

An enzyme activity assay was performed using a suspension of *Micrococcus lysodeikticus* cells in phosphate buffer at pH 7.0. The supernatant of the pooled samples were analyzed. The results of the assay, given as  $\Delta A_{450}/\text{min}$ , are given in Table 3.6.

Table 3.6: Assay results of the pooled supernatant samples.

Samples	$\Delta A_{450}/\text{min}$
Colony 1 , pooled 24hr samples, pH 6.0	0.002501
Colony 4 , pooled 24hr samples, pH 6.0	-0.003497
Colony 1 , pooled 24hr samples, pH 7.0	0.001886
Colony 4 , pooled 24hr samples, pH 7.0	0.004371
Colony 1, pooled samples, pH 6.0	0.004551
Colony 4, pooled samples, pH 6.0	0.002527
Colony 1, pooled samples, pH 7.0	-0.000152
Colony 4, pooled samples, pH 7.0	0.004191

## CHAPTER 4: DISCUSSION

Reactive oxygen species (ROS) are molecules or radicals produced from oxygen. Most ROS are highly reactive due to the presence of unpaired electrons in their valence shell. Metal ions such as  $\text{Fe}^{2+}$  or  $\text{Cu}^+$  are used as reducing agents in metal catalyzed oxidation (MCO) systems that generate the hydroxyl radical in a reaction with hydrogen peroxide. This is a highly reactive radical which oxidizes biological molecules at diffusion controlled rates. Many diseases such as rheumatoid arthritis, hemorrhagic shock, Parkinson's disease have been correlated to oxidation of proteins.

The purpose of this study was to create a site directed mutant of HEWL and insert the mutant gene into the *P. pastoris* genome. This was followed by small scale expression of the mutant protein. The N103H HEWL mutant gene was inserted into the pPICZ $\alpha$ A yeast vector. The pPICZ $\alpha$ A recombinant plasmid was linearized using restriction enzymes XhoI and XbaI, followed by the ligation of the N103H gene using the Quick Ligation Protocol™ from New England BioLabs. Ligation of N103H into pPICZ $\alpha$ A plasmid was confirmed by the viability of the colonies on Zeocin™ containing plates and by the double digest of the recombinant DNA using XhoI and XbaI restriction enzymes, followed by agarose gel electrophoresis. Gel electrophoresis revealed the presence of the N103H gene at 400 bp and the presence of a band at 3.6 kbp corresponding to the pPICZ $\alpha$ A plasmid. The recombinant plasmid with the N103H gene was linearized using BstX1 restriction enzyme. A subsequent analysis by agarose gel electrophoresis revealed linearization of the plasmid.

Different methods were tried to transform *P. pastoris* with the recombinant DNA. Various methods at generating competent yeast cells were tried. The cells were treated

using a solution containing 100 mM lithium chloride, 0.6 M sorbitol, 10 mM dithiothreitol and 10 mM Tris-HCl at pH 7.5 and a variant of the above solution using 100 mM lithium acetate. Preparation of chemically competent cells using 1 M sorbitol proved to be successful. The cells were transformed by electroporation at 1.5 kV, 25  $\mu$ F and 186  $\Omega$ . Integration of the recombinant plasmid into the yeast genome was evident with the growth of cells on YPDS plates containing Zeocin<sup>TM</sup>. Transformation was again confirmed by PCR screening which was done using Promega Master Mix<sup>TM</sup>, 5' AOX1 and 3' AOX1 primers (10  $\mu$ M). Subsequent analysis of the PCR products by 1% agarose gel electrophoresis showed two bands of which one confirms the presence of a gene of the right size and other band confirmed the Mut<sup>+</sup> phenotype.

Buffered medium was initially used for small scale expression. Small scale expression consists of an overnight growth in the presence of glycerol. The yeast was then switched to a growth medium that contained methanol as the only carbon source. In this study buffered minimal glycerol complex medium and buffered minimal methanol complex medium were used at pH 6.0. The transformed yeast expressed protein, with an overnight growth in BMGH medium followed by a growth in BMMH medium over a period of 96 hours (4 days). Expression of extracellular protein from either colony 1 or colony 4 of transformed X-33 was minimal (Figure 3.11). Expression from colony 4 was slightly better than from colony 1.

A second trial was performed where the buffered media was prepared with biotin prepared in 0.05M NaOH. In addition, 0.005% of antifoam 204 was used to prevent foaming and facilitate sufficient aeration. Media recipes in the scientific literature suggested the preparation of biotin in 0.05M NaOH.<sup>34</sup> Buffered methanol medium at pH

6.0 and at pH 7.0 were used for the second trial. The second trial was performed at 250 rpm at 30 °C and the samples were collected at 12 hour time intervals. The supernatant fractions were analyzed by SDS-PAGE. Both colonies of transformed X-33 showed much better expression of extracellular yeast proteins compared to the first trial. The molecular weight of one band was determined to be approximately 14.4 kD. This is close to the expected mass of the N103H HEWL mutant of 14.3 kD. Overall protein expression appears to be better at pH 7.0 (Figure 3.12 B) than at pH 6.0 (Figure 3.12 A).

The Bradford assay was performed to determine the concentration of protein in the supernatant fractions. Bovine serum albumin (BSA) was used to prepare the standard curve. The 24 hr samples were pooled and concentrated to measure the protein concentration using centrifugal concentrators. Total protein concentration for each sample was approximately 0.1 mg/mL (Table 3.4). An activity assay of the fractions showed no significant lysozyme activity. This was likely due to the low concentration of mutant protein present in the supernatant samples. In an effort to increase the concentration of the expressed proteins, all fractions were pooled and concentrated. A Bradford assay showed no significant increase in total protein concentration (Table 3.5). An enzyme assay of the concentrated supernatant fractions showed no significant lysozyme activity.

To rule out the presence of proteases in the supernatant fractions another trial of small scale expression with unbuffered minimal media was performed. The use of unbuffered media allows the pH drop to as low as 3.0 which inhibits protease activity. However, SDS-PAGE showed no evidence of extracellular expression of the proteins over 96 hrs (Figure 3.14).

## CHAPTER 5: CONCLUSION

The purpose of this project was to generate a site-directed mutant of lysozyme to study MCO systems and the site-specific oxidation of proteins. The mutant N103H gene was ligated into pPICZ $\alpha$ A and transformed into *E. coli*. The linearized recombinant DNA was used to transform the X-33 strain of *Pichia pastoris* by electroporation. PCR confirmed the integration of the recombinant DNA into the *Pichia* genome and the phenotype. Buffered media at pH 7.0 with the use of antifoam (0.005% v/v) and biotin prepared in 0.05 M NaOH were the best conditions for the extracellular expression of proteins.

Future work for this project involves the large scale expression and purification of the mutant lysozyme followed by oxidation studies. These oxidation studies will use the MCO system Cu(II) and H<sub>2</sub>O<sub>2</sub>. The oxidized N103H mutant will be studied for activity and its sites of oxidation will be determined by tandem mass spectrometry. These results will be compared to the oxidation pattern of the native HEWL enzyme in an effort to determine what relationship exists between site specific oxidation and the structure of a protein.

## REFERENCES

- 1) Bandyopadhyay, U., Das, D., and Banerjee, R.K. (1999) *Curr. Sci. India.* **77**, 658-666.
- 2) Turrens, J.F. and Boveris, A. (1980) *Biochem. J.* **191**, 421-427.
- 3) Reuter, S., Gupta, S.C., Chaturvedi, M.M., Aggarwal, B.B. (2010) *Free Rad. Bio. Med.* **49**, 1603-1616.
- 4) Fenton, H.J.H. (1984) *J. Chem. Soc. Trans.* **65**, 899-911.
- 5) Kehrer, J. P. (2000) *Toxicology.* **149**, 43-50.
- 6) Berlett, B.S. and Stadtman. (1997) *E.R. J. Biol. Chem.* **272**, 20313-20316.
- 7) Halliwell, B. (2009) *Free Rad. Bio. Med.*, **46**, 531-542.
- 8) Vellareddy, A., Kanthasamy, A., Choi, C.J., Martin, D.P., Latchoumycandane, C., Richt, J.A., Kanthasamy, A.G. (2008) *Free Rad. Bio. Med.* **45**, 1530-1541.
- 9) Stadtman, E.R. (1990) *Free Rad. Bio. Med.*, **9**, 315-325.
- 10) Stadtman, E.R. and Oliver, C.N. (1991) *J. Biol. Chem.* **266**, 2005-2008.
- 11) Hussain, S.P., Aguilar, F., Amstad, P. and Cerutti, P. (1994) *Oncogene.* **9**, 2277-2281.
- 12) Stadtman, E.R. and Levine, R.L. (2003) *Amino Acids.* **25**, 207-218.
- 13) Stadtman, E.R. and Berlett, B.S. (1997) *Chem. Res. Toxicol.* **10**, 485-494
- 14) Davies, M.J. (2005) *Biochim. Biophys. Acta.* **1703**, 93-109.
- 15) Stohs, S.J. and Bagchi, D. (1995) *Free Rad. Bio. Med.* **18**, 321-336.
- 16) Callewaert, L. and Michiels (2010) *C.W., J. Biosci.* **35**, 127-160.
- 17) Halliwell, B. (2009) *Free Rad. Bio. Med.* **46**, 531-542.
- 18) Canfield, R.E. and Liu, A.K. (1965) *J. Biol. Chem.* **240**, 1997-2002.
- 19) Voet, D. and Voet, J. (2011) "Biochemistry", John Wiley & Sons Inc. **4**, 517-525.

- 20) Chang, S.H., Teshima, G.M., Milby, T., Castro, B.G., Davis, E.C. (1997) *Anal. BioChem.* **244**, 221-227.
- 21) Ugrankar, M.M., Krishnamoorthy, G., and Prabhananda, B.S. (1991) *J. Biosci.* **16**, 21-28.
- 22) Shugar, D. (1952) *Biochim. Biophys. Acta.* **8**, 302-309
- 23) Khan, A.U. and Kasha, M. (1994) *Proc. Natl. Acad. Sci.* **91**, 12365-12367.
- 24) Gutteridge, J.M.C. and Halliwell, B. (2010) *Biochem. Biophys. Res. Commun.* **393**, 561-564.
- 25) Schoneich, C. and Williams, T.D. (2002) *Chem. Res. Toxicol.* **15**, 717-722.
- 26) Kambale, N.A. and Potdar, V.V. (2012) *Bionano Frontier.* **5**, 272-275.
- 27) Allen, R.G. and Tresini, M. (2000) *Free Rad. Bio. Med.* **28**, 463-499.
- 28) Aitken, R.J., Clarkson, J. S. and Fishel, S. (1989) *Biol. Reprod.* **40**, 183-197.
- 29) Liu, Y., Fiskum, G. and Schubert, D. (2002) *J. Neurochem.* **80**, 780-787.
- 30) Han, D., Williams, E. and Cadneas, E. (2001) *Biochem. J.* **353**, 411-416.
- 31) Li, X., Fang, P., Mai, J., Choi, E.T., Wang, H., and Yang, X.F. (2013) *J. Hematol. Oncol.* **6**, 1-19.
- 32) Martindale, J.L. and Holbrook, N.J. (2002) *J. Cell. Physiol.* **192**, 1-15.
- 33) Guptasarma, P., Balasubramanian, D., Matsugo, S. and Saito, I. (1992) *Biochem.* **31**, 4296-4303.
- 34) <http://www.bioch.ox.ac.uk/aspsite/services/mediakitchen/recipebook.pdf>